1979

A knietic model fo the gas recycle hydrogenator

James M. Hanna
Lehigh University

A KINETIC MODEL OF THE GAS RECYCLE HYDROGENATOR

by

James M. Hanna

A Design Report

Presented to the Graduate Faculty

of Lehigh University

in Candidacy for the Degree of

Master of Science

in

Chemical Engineering

Lehigh University

1979

A KINETIC MODEL OF THE

GAS RECYCLE HYDROGENATOR

by

James M. Hanna

This design report is accepted and approved in partial fulfillment of the requirements for the degree of Master of Science.

May 9 1979
(date)

Fred P. Stein
Professor in Charge

Chairman of Department

ACKNOWLEDGMENTS

The Chemical Engineering Department of Lehigh University and Air Products and Chemicals, Inc. must be sincerely thanked for providing both the opportunity to participate in the M.S. Design Option Program, and the financial support needed to continue graduate education. Additional appreciation is extended to Air Products for the use of their facilities and for the opportunity to interact with some high-caliber professionals.

Without the ideas, enthusiasm and "open ears" of Mr. Joe Klosek and Dr. Edward M. Phillips of Air Products, this author could never have lasted the summer. Acting as thesis advisor, Dr. Fred P. Stein served as an important bridge between the university and industrial environments. Constantly providing encouragement and advice, he was my third spark plug when progress was slow. I am most grateful to all three for their help and interest.

I am also appreciative of the efforts of Dr. Kem Anselmo who provided the numerical analysis techniques utilized in this thesis. Finally, I would like to both thank and apologize to my family (especially by brothers and sister), my three apartment roommates and my fellow graduate students who have put up with me at my "complaining best".

TABLE OF CONTENTS

Page

Title Page i

Certificate of Approval. ii

Acknowledgments. iii

Table of Contents. iv

List of Tables vi

List of Figures. vii

Abstract 1

Chapter

I. INTRODUCTION. 2

II. DESCRIPTION OF THE GAS RECYCLE HYDROGENATOR 4

III. EXTENSION OF THE WEIMER GRH KINETIC MODEL 6

A. Background. 6

B. Weimer's Original Model 8

1. Simplifying Assumptions. 8

2. The Kinetic Model. 9

3. Initial Breakdowns 13

4. Reaction Rate Expressions. 13

C. Modification of Weimer's Model: Initial Breakdown Correlations. 16

1. Characteristic Initial Breakdowns. 16

2. Development of Correlations. 16

3. Parity Plots 27

4. Mass Balances. 38

5. Temperature Effects. 40

Page

D. Summary. 45

E. Recommendations. 47

IV. FIRST-PRINCIPLES APPROACH. 48

A. Introduction 48

B. Numerical Analysis Methods 50

C. Kinetic Models for the Hydrogenolysis of Paraffins . . 52

1. Literature Data 52

2. Ethane Hydrogenolysis 52

3. Propane Hydrogenolysis. 57

4. Effects of Hydrogen Partial Pressure. 58

5. n-Butane Hydrogenolysis 62

D. Summary. 73

References. 75

Appendix

A. Sample Calculations. 77

B. GRH Hydrogasification Data 81

C. Location of Hydrogasification Data in the References . 94

LIST OF TABLES

Table		Page
1.	Reaction Rate Parameters	15
2.	Characteristic Initial Breakdowns	17
3.	Mathematical Expressions for Initial Breakdown Correlations	29
4.	Feedstock Plotter Symbols	30
5.	Ethane Hydrogenolysis	55
6.	Propane Hydrogenolysis	59
7.	Propane Hydrogenolysis - Effects of Pressure	64
8a.&b.	n-Butane Hydrogenolysis	70
9.	Kinetic Rate Constants for the n-Butane Hydrogenolysis Runs	72
B-1.	Hydrogasification of Butane, Synthetic Fuel (SF) and Natural Gas Condensate (NGC)	81
B-2.	Hydrogasification of LDF 115	82
B-3a.&b.	Hydrogasification of LDF 170	83
B-4.	Hydrogasification of Kerosene	85
B-5a.&b.	Hydrogasification of No. 2 Fuel Oil	86
B-6.	Hydrogasification of Diesel Oil	88
B-7a.&b.	Hydrogasification of Topped Kuwait Crude Oil Fraction	89
B-8.	Hydrogasification of Monagas Crude Oil Fraction	91
B-9a.&b.	Hydrogasification of Athabasca Tar Sands Crude Oil Fraction	92

LIST OF FIGURES

Figure		Page
1.	The Operating Principle of the Gas Recycle Hydrogenator	5
2.	GRH Reaction Mechanism.	10
3.	Component Mass Balances	12
4.	Initial Breakdown Correlation	20
5.	Initial Breakdown Correlation	21
6.	Initial Breakdown Correlation	22
7.	Initial Breakdown Correlation	23
8.	Initial Breakdown Correlation	24
9.	Initial Breakdown Correlation	25
10.	W_1 (Methane) Parity Plot.	31
11.	W_2 (Ethane/Ethylene) Parity Plot.	32
12.	W_3 (Propane/Propylene +) Parity Plot.	33
13.	W_4 (BTX) Parity Plot.	34
14.	W_5 (Naphthalene) Parity Plot.	35
15.	W_6 (Anthracene) Parity Plot	36
16.	Initial Breakdown Temperature Effects	43
17.	Initial Breakdown Temperature Effects	44
18.	Least Squares Fit of Ethane Hydrogenolysis Rate Constant (K_1)	56
19.	Least Squares Fit of Propane Hydrogenolysis Rate Constant (K_2)	60
20.	Propane Hydrogenolysis: 1st order vs. 2nd order.	63
21.	Kinetic Model of n-Butane Hydrogenolysis.	66

ABSTRACT

An existing kinetic model of the Gas Recycle Hydrogenator (GRH) was extended to provide the capability of predicting reactor yield and product distribution, provided that the feedstock parameters of molecular weight and carbon/hydrogen weight ratio are known. In developing the necessary correlations required to determine the effluent composition, a data set consisting of numerous GRH runs under various conditions was incorporated into the model. The various feedstocks to the GRH included butane, kerosene, diesel oil, a synthetic fuel oil, No. 2 Fuel Oil, two light distillate fractions whose boiling endpoints are approximately 115 and 170°C, a natural gas condensate and the partially vaporized crude oils Athabasca Tar Sands, Topped Kuwait and Monagas. For each of the GRH runs in the data set, the product distribution in the form of seven specific groups, each consisting of similar hydrocarbon compounds, was predicted, and these values were compared to observed results. The model's accurate predictions of the alkane/alkene effluent yields, particularly methane and ethane/ethylene which account for over 70% of the product, by weight, were in sharp contrast to its weakness in predicting the product distribution for the aromatic compounds.

In an attempt to predict the effluent yields in terms of individual molecular species rather than "lumped" groups, an alternate modeling approach was considered. However, limited results in combination with a target date for a completed model did not justify an exhaustive study of this alternative.

I. INTRODUCTION

The Chemical Engineering Department of Lehigh University, in cooperation with local industry, offers a design option to M.S. candidates desiring special experience in engineering design. This thesis topic concerning the Gas Recycle Hydrogenator was proposed by Air Products and Chemicals, Inc. of Allentown, Pennsylvania and was pursued as part of the M.S. Design Option Program. The author has conducted his research within Air Products' Process Engineering Department under the supervision of Mr. Joseph Klosek and Dr. Edward M. Phillips of the Management Information Department. The third member participating in the supervision of this research project was Dr. Fred P. Stein of Lehigh University. The proposed project involves the development of a kinetic model for the Gas Recycle Hydrogenator (GRH).

The GRH was developed by the British Gas Council (presently the British Gas Corporation) at their Midlands Research Station in Solihull, England. This process of non-catalytic hydrogenation of hydrocarbon feedstocks was first described in 1963 [15]. The original application of the GRH reactor was for the enrichment of Lurgi gas [15, 16]. Currently, Air Products has adapted British Gas Corporation's (BGC) GRH technology for the production of substitute natural gas and petrochemical feedstocks from high sulfur gas oils [14].

The rapid depletion of the supply of natural gas in the United States coupled with the Department of Energy's restriction that light distillates, such as naphtha, be utilized only as petrochemical feedstocks has spurred the company's interest in GRH technology. The GRH reactor has the potential to gasify feedstocks of increased boiling end points from 400 to 650°F [16]. The gasification of middle distillate fractions (650°F end points) offers a significant cost advantage over the restricted naphtha.

Although Air Products has spent considerable effort in developing GRH technology, there was no in-house fundamental framework describing reactor kinetics which would make possible the a priori prediction of the effluent compositions, given reactor operating conditions and a feedstock analysis. BGC has empirical correlations which are based upon light distillate feedstocks and moderate reactor temperatures. To extend these correlations to the operating conditions at which Air Products intends to run the GRH (i.e., middle distillate feedstocks and/or higher reactor temperatures), extrapolation and engineering judgment were employed by BGC. To aid in both the understanding of GRH performance and in the assessment of the applicability of these extrapolations from empirical correlations, a model of GRH kinetics needed to be developed. This research project is an attempt to satisfy this need.

II. DESCRIPTION OF THE GAS RECYCLE HYDROGENATOR [16, 19]

The Gas Recycle Hydrogenator, shown in Figure 1, consists of a cylindrical reaction vessel with a coaxial draft tube inside. A mixture of hydrogenating gas and hydrocarbon feedstock is injected into the draft tube through a feed nozzle. The high velocity of the inlet jet induces the reactants to circulate down the inner tube and up the annulus. This rapid recirculation causes the inlet gases to mix with a relatively large amount of hot gases, whereby they absorb the exothermic heat of reaction. Hence, the inlet gases quickly reach reaction temperature. Except for locations close to the feed nozzle, close control of reactor temperature can be achieved, within a few degrees, by allowing for an adequate recirculation rate. Pilot plant studies have revealed recirculation ratios (volume of recirculating gas per volume of inlet gas) of more than 10:1. Determining factors of the recirculation rate are:

1. Ratio of draft tube diameter to that of nozzle jet.
2. Ratio of the reactor temperature to that of the inlet gases.
3. Resistance to flow of the recirculating gases.

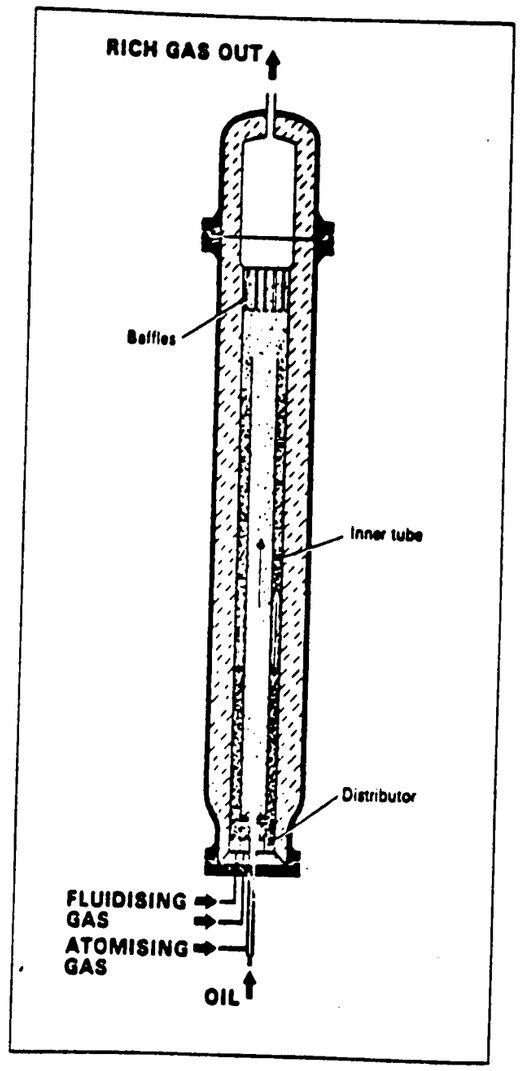

FIGURE 1

THE OPERATING PRINCIPLE OF THE GAS RECYCLE HYDROGENATOR

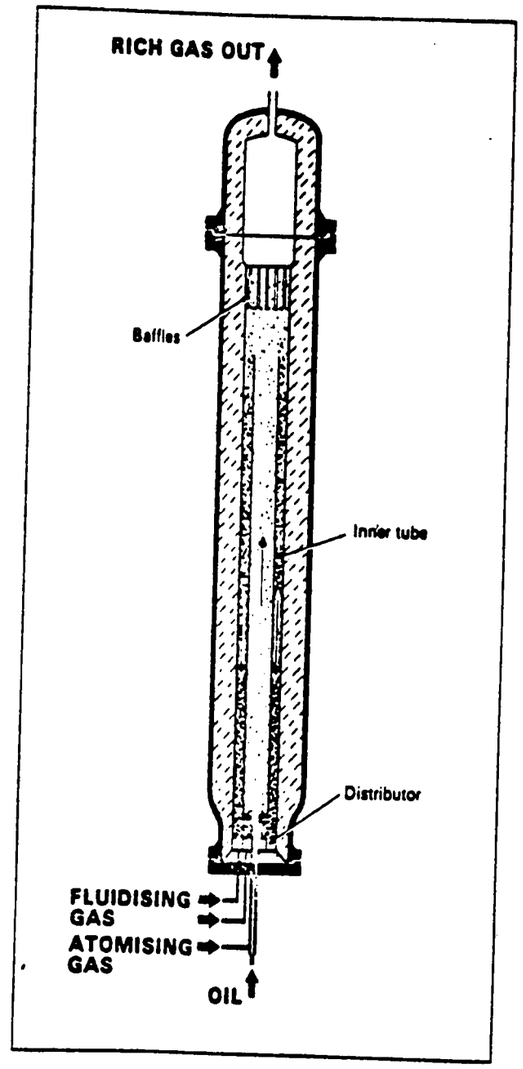

FIGURE 1

THE OPERATING PRINCIPLE OF THE GAS RECYCLE HYDROGENATOR

III. EXTENSION OF THE WEIMER GRH KINETIC MODEL

A. Background

In 1977 R. F. Weimer [21] proposed a hydropyrolysis model in an effort to describe the reaction kinetics which occur inside the GRH reactor. The key assumption of this model is that the hydrocarbon feedstock, upon entering the GRH, instantaneously decomposes into seven "lumped" hydrocarbon groups known as the initial breakdown. This initial breakdown then further reacts, in the presence of a large excess of hydrogen, to yield the effluent components.

Weimer stipulated that the initial breakdown was independent of reactor temperature and that each feedstock had its own characteristic initial breakdown. These characteristic breakdowns were back calculated from existing pilot plant and laboratory data, and effluent yields were then predicted. The initial results were encouraging and Weimer felt that the model provided a gross, qualitative description of GRH kinetics.

Since the inception of this simplified hydropyrolysis model, an enlarged data set has been made available. The purpose of this part of the study is threefold:

1. The additional data will be incorporated into the model.
2. An attempt will be made to correlate these characteristic initial breakdowns with parameters that define the feedstock character.
3. The effect of both reactor and preheater temperature on the initial breakdown will be analyzed.

B. Weimer's Original Model

1. Simplifying Assumptions

Weimer's simple hydropyrolysis model [21] of GRH kinetics accounts for the effects of reactor temperature and residence time. The model rests upon several simplifying assumptions:

a. The feedstock hydrocarbons crack only into smaller compounds.

b. The reverse reactions, i.e., equilibrium, are neglected as are any polymerization or dehydrogenation reactions (e.g., $C_2H_6 = C_2H_4 + H_2$).

c. Upon entering the GRH, the feedstock instantaneously undergoes an initial breakdown into seven classes of hydrocarbons. These "lumped" groups are:

C_1	methane
C_2	ethane, ethylene
C_3	propane, propylene and heavier paraffins
A_1	benzene, toluene and xylene
A_2	naphthalene and similar two-ring aromatic compounds
A_3	anthracene and similar three-ring aromatic compounds
A_4	pyrene and similar four-ring aromatic compounds

d. The initial breakdown is independent of reactor operating conditions such as reactor temperature and pressure. This breakdown is characteristic only of the particular feedstock entering the GRH.

e. With the exception of methane, each "lumped" group of this instantaneous initial breakdown hydropyrolyzes via first-order, rate controlled reactions to yield the GRH effluent. The effect of hydrogen partial pressure on these reaction rates is ignored.

2. The Kinetic Model

After having undergone the initial breakdown, the feedstock, in the form of seven hydrocarbon groups, further reacts in the presence of a large excess of hydrogen to produce the GRH effluent components. The reaction mechanism is presented in Figure 2. C_i and A_i represent the amounts, by weight, of each of the seven hydrocarbon groups. The coefficients account for the approximate amount of hydrogen consumed by each reaction. Appendix A presents a sample calculation for arriving at these coefficients. The initial breakdown quantities are represented by X_i's while the effluent quantities are denoted by W_i's, where $i = 1,2,\ldots,7$ represents hydrocarbon groups C_1, C_2, C_3, A_1, A_2, A_3 and A_4, respectively.

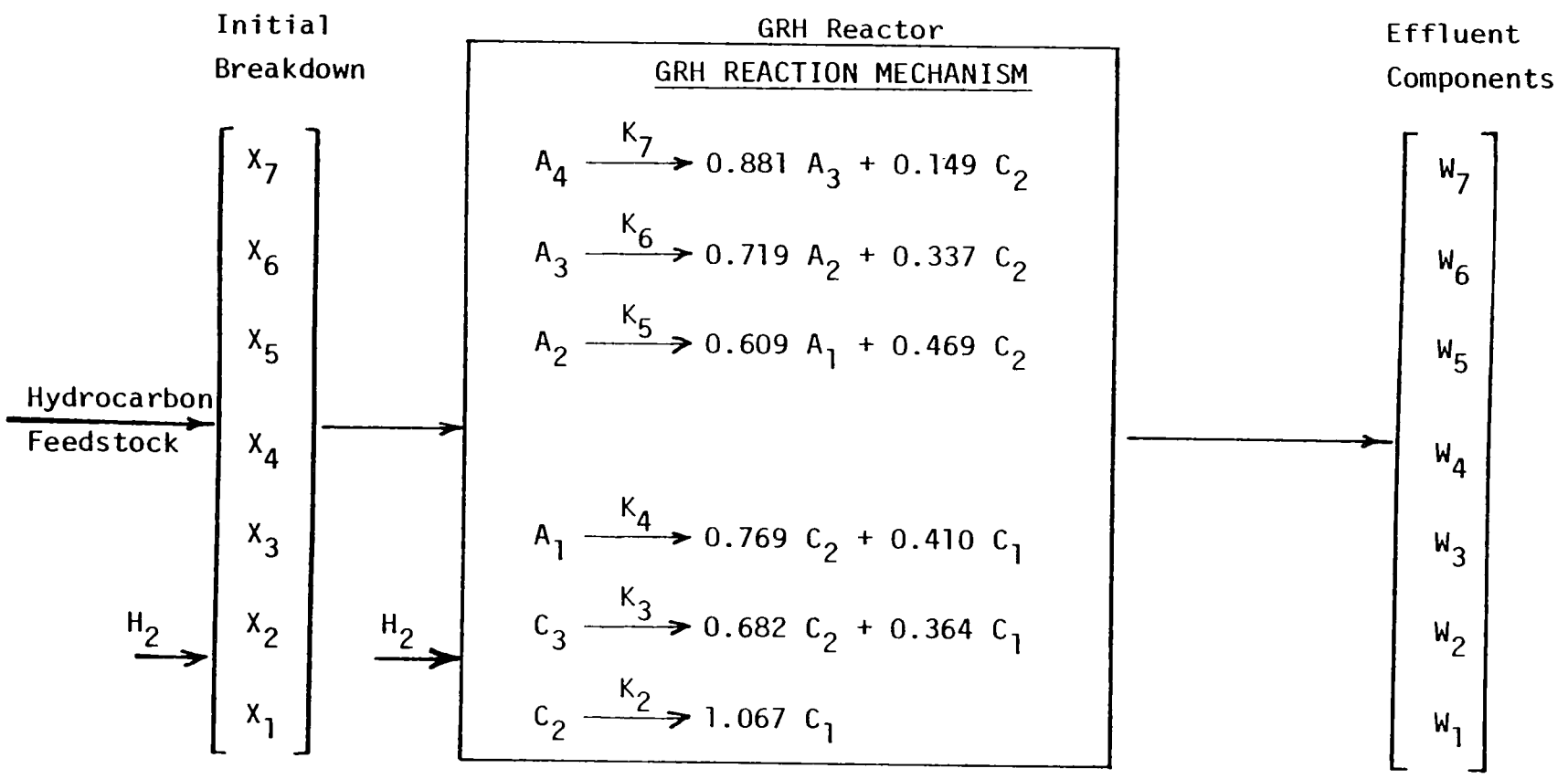

Figure 2. GRH Reaction Mechanism

The reaction scheme consists of six possible reactions; each reaction involving the hydropyrolysis of a hydrocarbon group into hydrocarbon group(s) of lower molecular weight. Except for the BTX* group (A_1), each aromatic group cracks into an aromatic group of one-less ring and the ethane-ethylene group (C_2). The BTX group hydropyrolyzes into the C_2 group and methane as does the C_3 group consisting of propane, propylene and heavier paraffins.

Because of a high internal recirculation rate, the GRH was simulated as a perfectly back-mixed reactor. When developing component mass balances for each of the hydrocarbon groups, the initial breakdown composition was considered to be the feed to this back-mixed reactor. The seven hydrocarbon groups which define the initial breakdown were assumed to hydropyrolyze via first-order, rate controlled reactions to yield the GRH effluent components. The resulting component mass balances, presented in Figure 3, give the amount, W_i, of each hydrocarbon group in the product in terms of pounds of product per pound of oil fed to the GRH. The GRH residence time is given by t_R, and the X_i's represent the quantity of each class of hydrocarbon formed during the assumed initial breakdown.

*Benzene, toluene and xylene

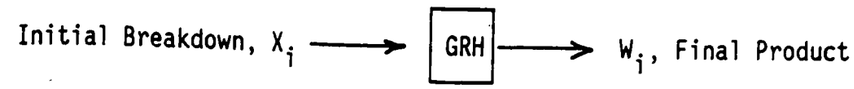

Hydrocarbon Group	Component Mass Balances
Pyrene	$W_7 = X_7/(1 + K_7 t_R)$
Anthracene	$W_6 = (X_6 + 0.881\ K_7 t_R W_7)/(1 + K_6 t_R)$
Naphthalene	$W_5 = (X_5 + 0.719\ K_6 t_R W_6)/(1 + K_5 t_R)$
BTX	$W_4 = (X_4 + 0.609\ K_5 t_R W_5)/(1 + K_4 t_R)$
C_3H_8, C_3H_6 +	$W_3 = X_3/(1 + K_3 t_R)$
C_2H_6, C_2H_4	$W_2 = (X_2 + 0.149\ K_7 t_R W_7 + 0.337\ K_6 t_R W_6 + 0.469\ K_5 t_R W_5 + 0.769\ K_4 t_R W_4 + 0.682\ K_3 t_R W_3)/(1 + K_2 t_R)$
CH_4	$W_1 = X_1 + 0.410\ K_4 t_R W_4 + 0.364\ K_3 t_R W_3 + 1.067\ K_2 t_R W_2$

Figure 3. Component Mass Balances

3. Initial Breakdowns

The Weimer hydropyrolysis model rests upon the major assumption that the oil feed, upon entering the GRH, immediately and instantaneously undergoes an initial breakdown into seven specific hydrocarbon groups. These initial breakdown components then hydrogenate via first-order, rate controlled reactions to yield the final product. Knowledge of the product composition, reactor temperature and residence time allows for the back calculation of this assumed initial breakdown. Appendix B tabulates the initial breakdowns for the numerous pilot plant and laboratory runs that have been analyzed. The various feedstocks to the GRH are butane, a synthetic fuel oil, diesel oil, kerosene, a natural gas condensate, LDF 115 and LDF 170 (two light distillate fractions whose boiling end points are about 115 and 170°C, respectively), No. 2 Fuel Oil and the partially vaporized crude oils: Athabasca Tar Sands, Topped Kuwait and Monagas.

4. Reaction Rate Expressions

In presenting a GRH kinetic model, Weimer also proposed a set of reaction rate expressions. These expressions have their origins in the thermal hydrogenolysis literature and had been altered by Weimer so as to predict GRH product yields with greater accuracy [21]. Since Weimer's original proposal, an enlarged

data set had been made available, necessitating a further adjustment of the pre-exponential factors in order to achieve better agreement with the new data. Table 1 lists these reaction rate parameters.

Table 1. Reaction Rate Parameters

Kinetic Rate Constant	Weimer's Parameters		Hanna's Modified Parameters
	Pre-exponential Factor	Activation Energy (Btu/lb mol)	Pre-exponential Factor
K_2	1.5×10^{13}	126,500	1.5×10^{13}
K_3	8.0×10^{10}	93,500	8.0×10^{10}
K_4	7.92×10^{8}	94,700	8.8×10^{8}
K_5	20.25×10^{5}	66,200	30.25×10^{5}
K_6	3.6×10^{5}	55,300	1.8×10^{5}
K_7	6.8×10^{5}	60,300	6.8×10^{5}

C. Modification of Weimer's Model: Initial Breakdown Correlations

1. Characteristic Initial Breakdowns

After calculating the initial breakdowns for the available pilot plant and laboratory runs, a key observation was made. The initial breakdowns did not vary substantially among the runs for any one feedstock, i.e., each feedstock can be characterized by an average initial breakdown. Table 2 lists the arithmetically-averaged initial breakdowns for the various feedstocks.

These average initial breakdowns were then used to calculate the effluent compositions. The predicted values showed reasonable agreement with observed results to lend credence to the theory that each feedstock possesses a characteristic initial breakdown. The next step was to correlate these characteristic initial breakdowns with parameters that define the feedstock.

2. Development of Correlations

In attempting to correlate the initial breakdown as a function of feedstock character, three criterion were considered. First, the correlating parameters which define the feedstock were to be readily available or easily determined. Secondly, simple parameters would be preferred to complex parameters. Although a complex parameter might provide a better correlation, a simple correlating parameter was deemed more desirable in

Table 2. Characteristic Initial Breakdowns

FEEDSTOCK	Butane	LDF 115	LDF 170	Natural Gas Conden.	Kero-sene	No. 2 Fuel Oil	Diesel Oil	Topped Kuwait	Mongas (Run H-30)	Mongas	Tar Sands	Syn-thetic Fuel
FEEDSTOCK PARAMETERS								70% Fraction	25% Fraction	50% Fraction	55% Fraction	
Carbon/Hydrogen Weight Ratio	4.75	5.31	5.66	5.90	6.09	6.49	6.49	6.61	6.97	7.21	7.90	9.47
Molecular Weight	56.8	85.0	98.8	103	150	212	218	272	215	300	345	101
Specific Gravity	0.569	0.671	0.713	0.758	0.783	0.837	0.834	0.860	0.910	0.946	0.950	0.847
Volume % Aromatics	0	1.40	6.40	12.9	15.0	33.3	28.7	33.0	22.0	28.0	45.0	82.7
AVERAGE INITIAL BREAKDOWN lb/lb Hydrocarbon Feed												
X_1	0.308	0.166	0.272	0.329	0.190	0.253	0.198	0.210	0.383	0.396	0.405	0.070
X_2	0.452	0.368	0.432	0.416	0.262	0.396	0.274	0.443	0.099	0.259	0.248	0
X_3	0.257	0.430	0.230	0.100	0.398	0.094	0.292	0.115	0	0	0	0
X_4	0.010	0.056	0.100	0.178	0.128	0.104	0.105	0.149	0.301	0.178	0.210	0.723
X_5	0.001	0.001	0.004	0	0.040	0.118	0.048	0.024	0	0.004	0.062	0.106
X_6	0	0.013	0.008	0.059	0.020	0.009	0.226	0.062	0.261	0.178	0.007	0.005
X_7	0	0	0	0	0	0.042	0	0.008	0	0	0.026	0
CORRELATING GROUPS												
$X_1 + X_2 + X_3$	1.02	0.964	0.934	0.845	0.850	0.743	0.764	0.768	0.482	0.655	0.653	0.070
$X_2 + X_3$	0.709	0.798	0.662	0.516	0.660	0.490	0.566	0.558	0.099	0.259	0.248	0
$X_1 + X_3$	0.565	0.596	0.502	0.429	0.588	0.347	0.490	0.325	0.383	0.396	0.405	0.070
$X_4 + X_5 + X_6 + X_7$	0.011	0.070	0.112	0.237	0.188	0.273	0.379	0.243	0.562	0.360	0.305	0.834
$X_4/(X_4 + X_5 + X_6 + X_7)$	0.909	0.800	0.893	0.751	0.681	0.381	0.277	0.613	0.536	0.494	0.688	0.867
$(X_4 + X_5)/(X_4 + X_5 + X_6 + X_7)$	1.00	0.814	0.928	0.751	0.894	0.813	0.404	0.712	0.536	0.506	0.892	0.994

order to be consistent with the simplicity of the kinetic model. Finally, it was hoped that a physical explanation could be associated with each correlation. This criterion was the least enforced.

There are four feedstock parameters which are available for all of the existing data and which also satisfy the criterion of being easily determined. These defining parameters are carbon/hydrogen (C/H) weight ratio, specific gravity, molecular weight and aromatics content (volume %) of the feedstock. Of these, only the C/H weight ratio and molecular weight were utilized in the initial breakdown correlations. The correlating groups for the initial breakdown are $(X_1 + X_2 + X_3)$, $(X_2 + X_3)$, $(X_1 + X_3)$, $(X_4 + X_5 + X_6 + X_7)$, $X_4/(X_4 + X_5 + X_6 + X_7)$ and $(X_4 + X_5)/(X_4 + X_5 + X_6 + X_7)$. The values for the feedstock parameters and the initial breakdown correlating groups can be found in Table 2.

$(X_1 + X_2 + X_3)$, $(X_2 + X_3)$ and $(X_1 + X_3)$ exhibit linear relationships with the C/H weight ratio, and these linear functions are presented in Figures 4, 5 and 6, respectively. All three initial breakdown correlating groups decrease in value with increasing C/H weight ratios. The correlating group $(X_4 + X_5 + X_6 + X_7)$ is also a linear function of C/H

weight ratio, as shown in Figure 7. However, increasing C/H weight ratios result in larger $(X_4 + X_5 + X_6 + X_7)$ values.

The correlating groups $X_4/(X_4 + X_5 + X_6 + X_7)$ and $(X_4 + X_5)/(X_4 + X_5 + X_6 + X_7)$ are plotted as linear functions of molecular weight in Figures 8 and 9, respectively. These correlations exhibit the largest scatter in the data, especially the latter group. Both parameters decrease in value with increasing molecular weight.

For all feedstocks, the amount of the initial breakdown group X_7 is either zero or very small. For many of the runs, the reason for this virtual non-existence of X_7 stems from the lack of resolution in the effluent yield analysis for aromatics content. The aromatics analysis was broken down into groups such as benzene/toluene/xylene, naphthalene and higher aromatics. These higher aromatics were interpreted to be 3-ring aromatic compounds, i.e., effluent group W_6. The amount of 4-ring compounds (W_7) was assumed to be negligible [13]. Hence, the back calculation of the initial breakdown group X_7 would be zero. Therefore, only six of the initial breakdown groups remain to be predicted. The six proposed correlations make these

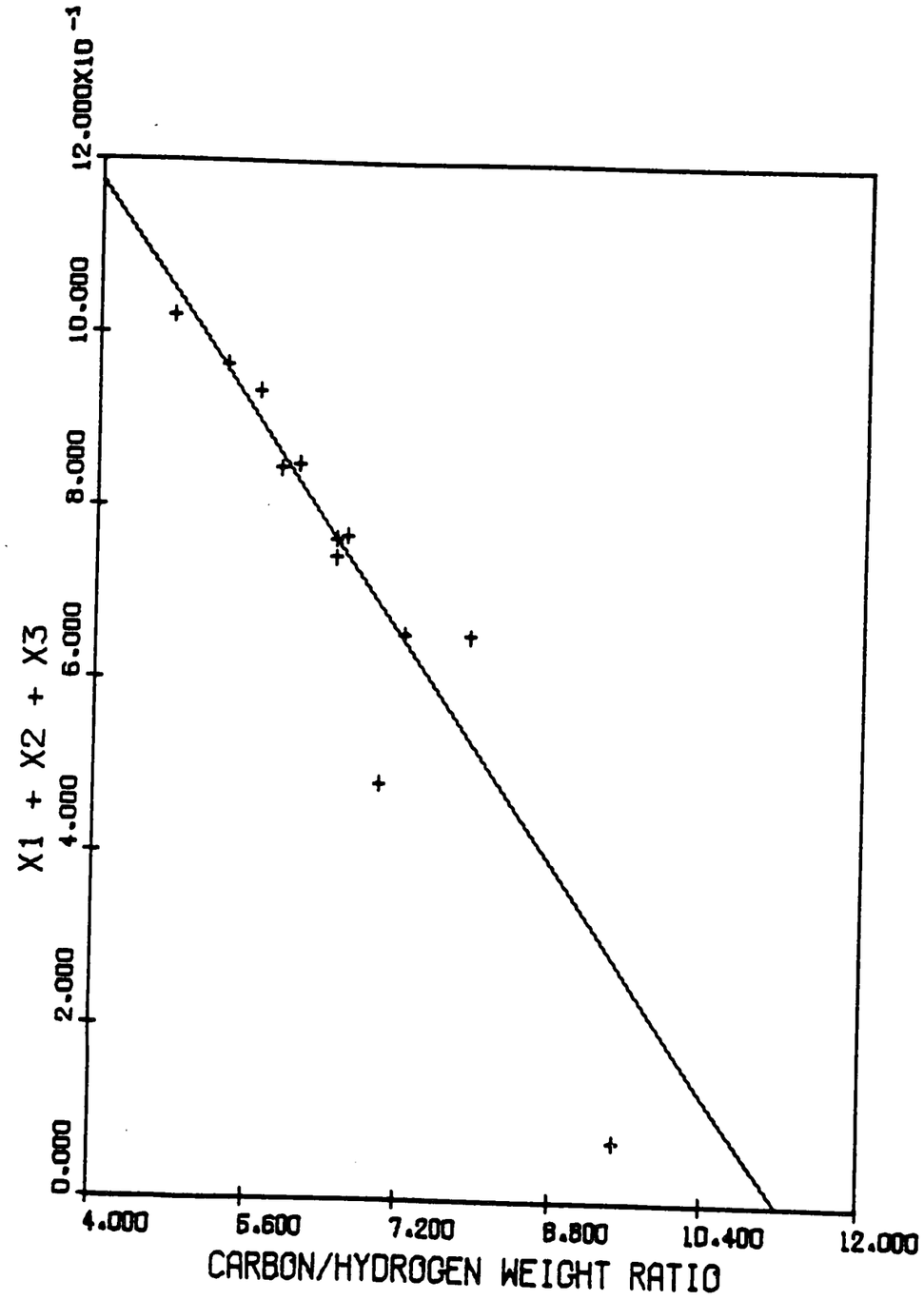

FIGURE 4

INITIAL BREAKDOWN CORRELATION

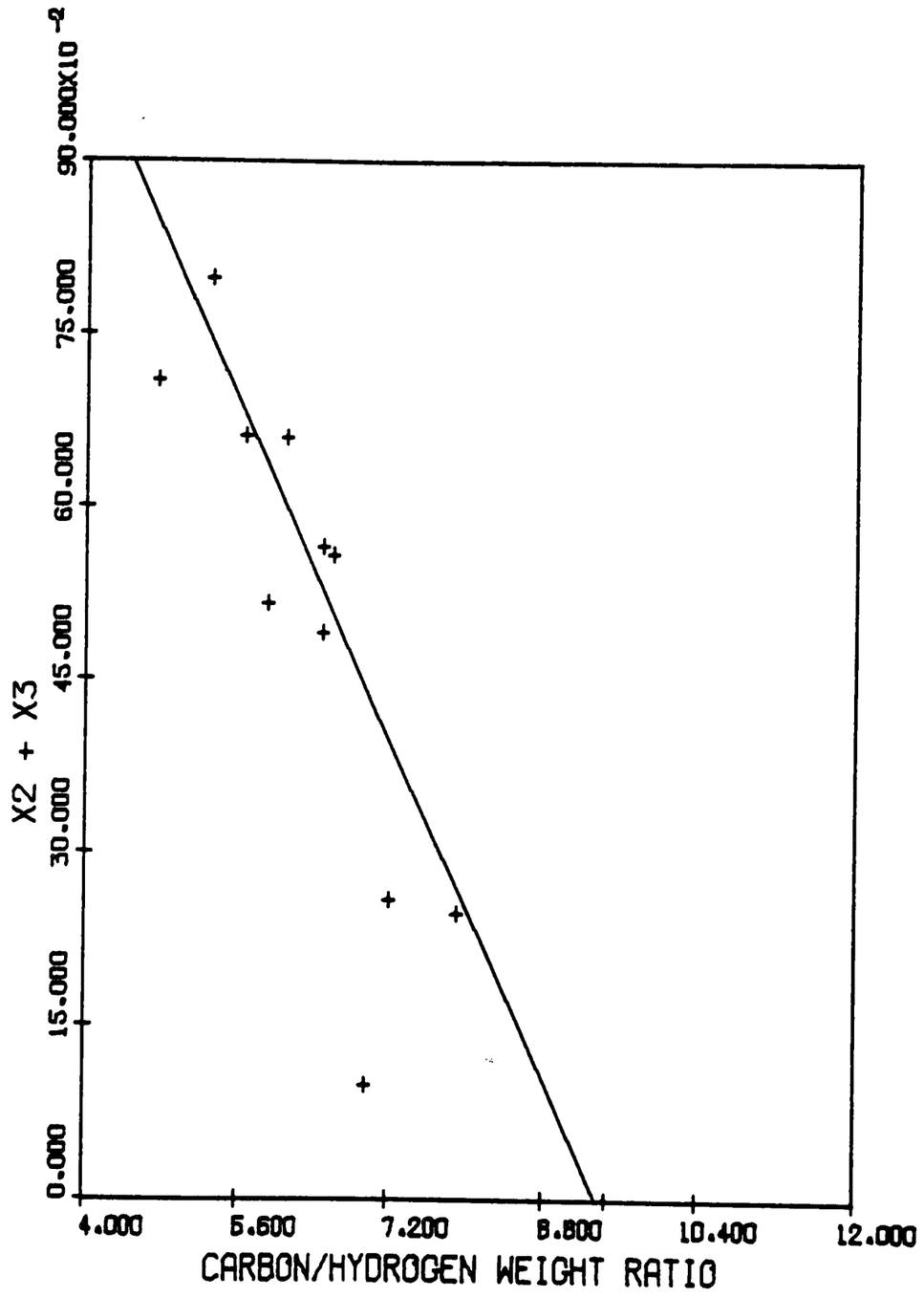

FIGURE 5

INITIAL BREAKDOWN CORRELATION

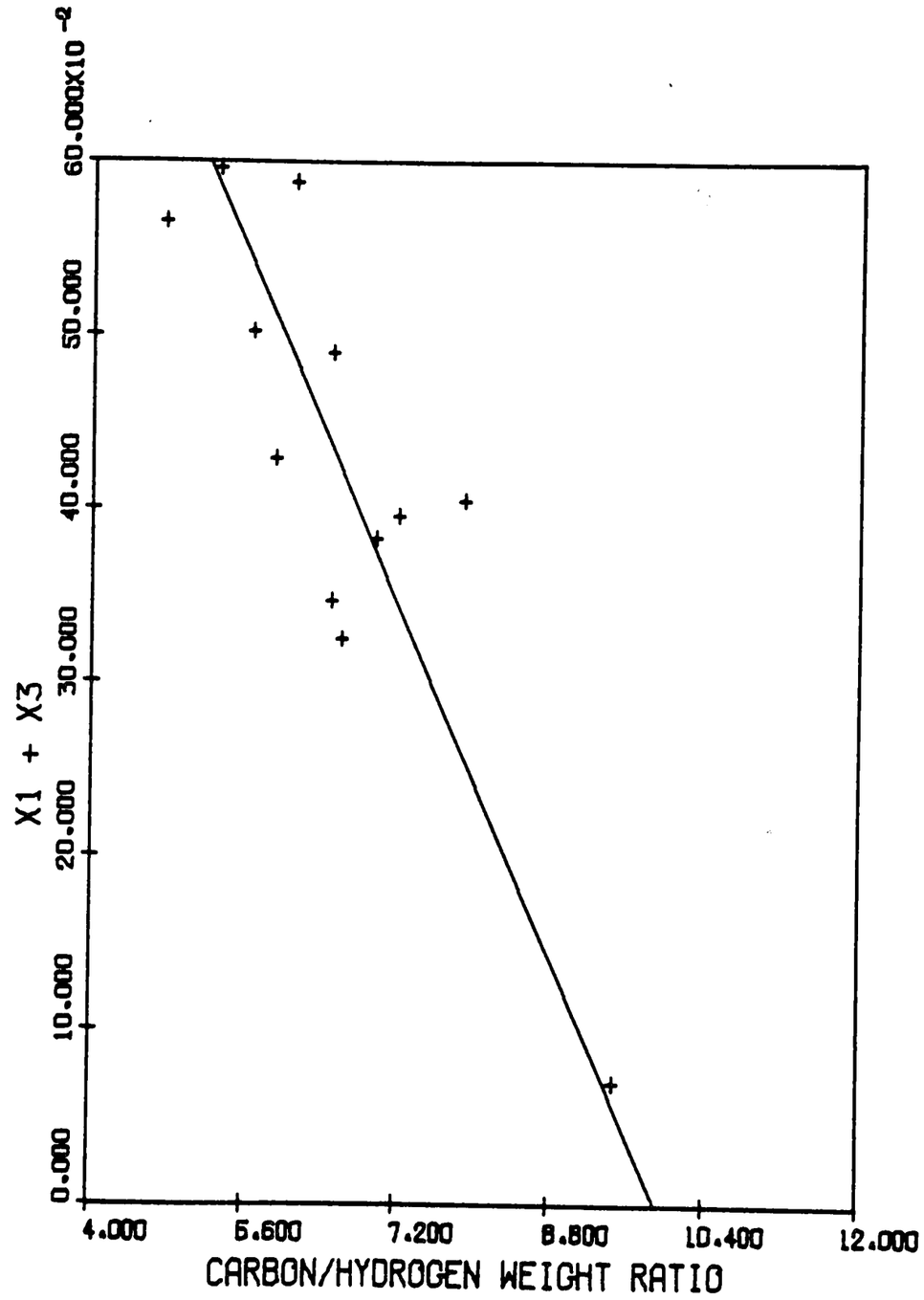

FIGURE 6

INITIAL BREAKDOWN CORRELATION

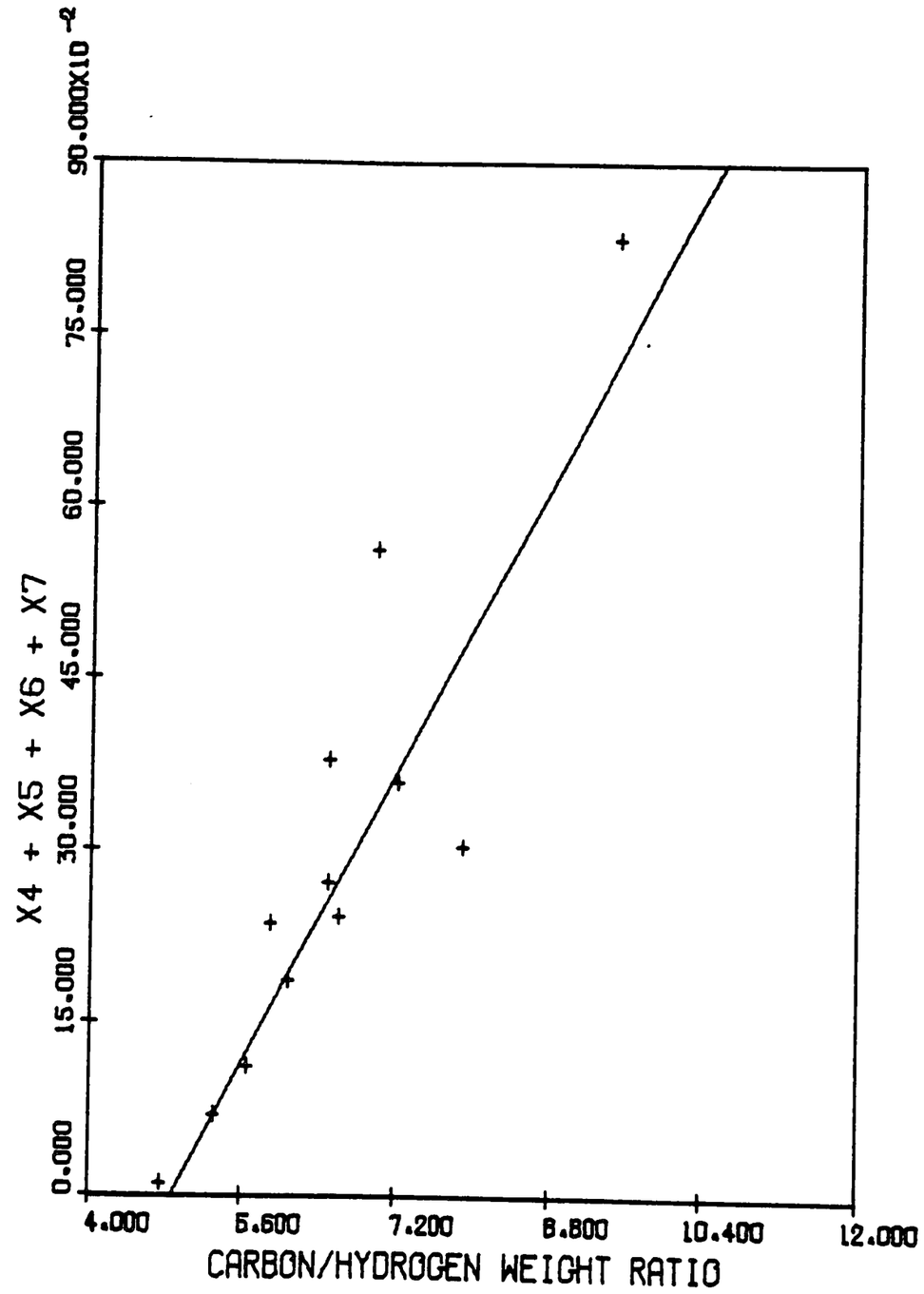

FIGURE 7

INITIAL BREAKDOWN CORRELATION

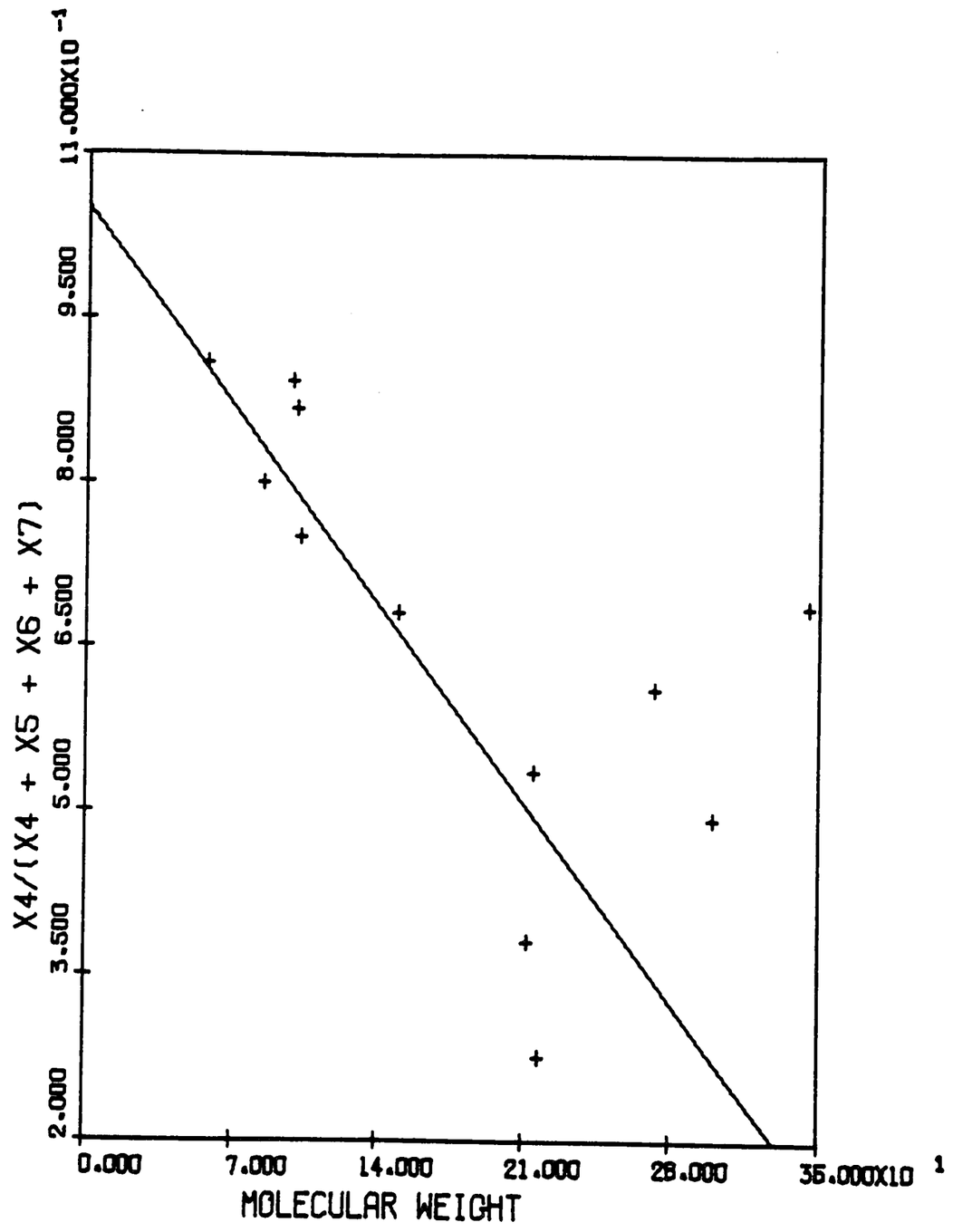

FIGURE 8

INITIAL BREAKDOWN CORRELATION

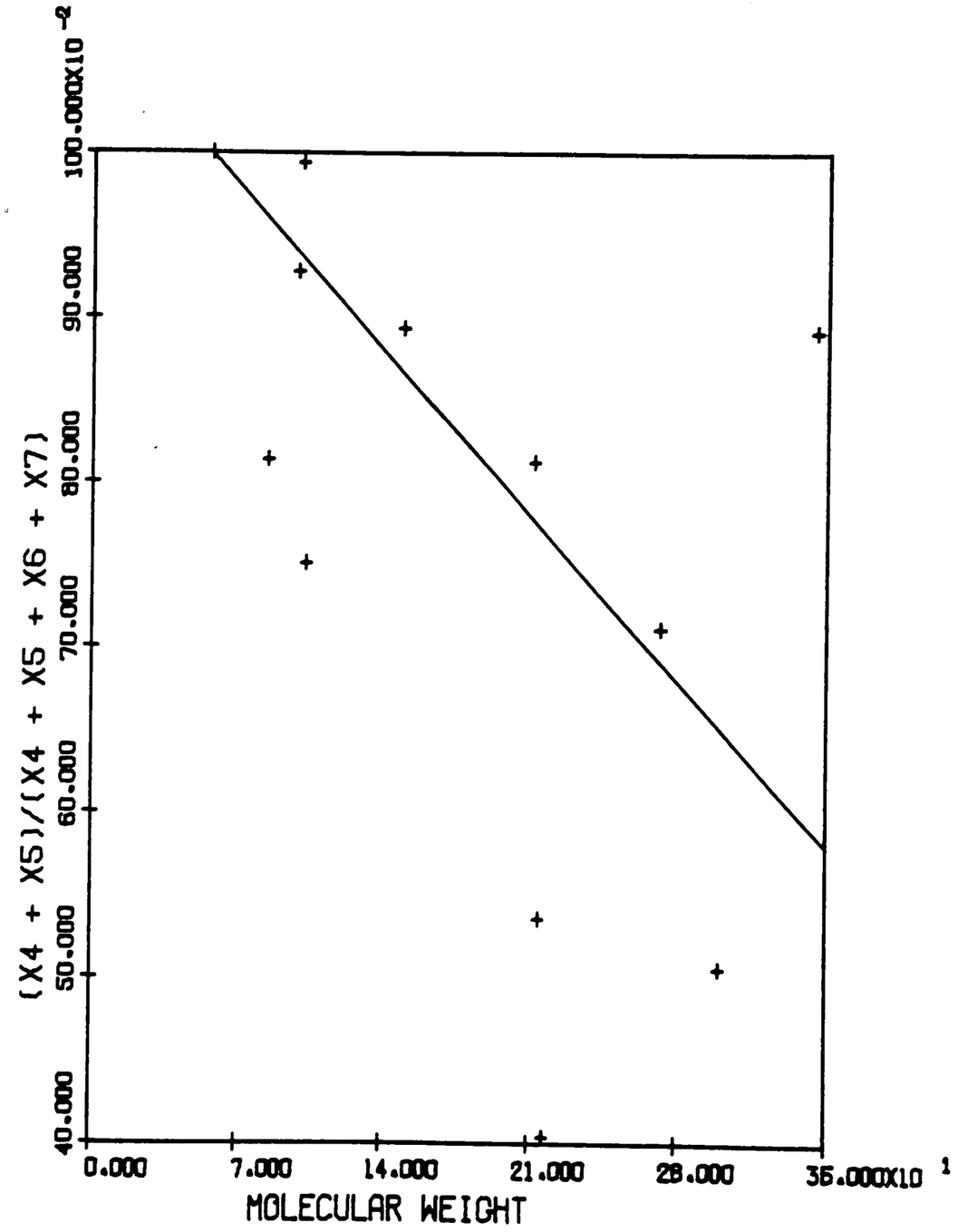

FIGURE 9

INITIAL BREAKDOWN CORRELATION

calculations possible [Figures 4-9].

The correlating lines do not represent least squares fits. The lines drawn are what the author feels are the "best" fits to the data. Each data point is an arithmetically-averaged value of a particular feedstock's GRH runs. The number of runs for each feedstock varies from one to ten. Because of the diverse nature of the feedstocks which range from pure butane to synthetic fuel, the assignment of weighting factors to each data point would be difficult. Not only must these factors reflect the number of runs involved in the average but also the qualitative answer to the validity of each feedstock's presence in the correlations. Therefore, a least squares fit may be as arbitrary as an estimated best fit.

Not surprisingly, the functions which best correlate the data are the same relationships for which a physical explanation can be offered. Relative to the other four correlations, the correlations of the groups $(X_1 + X_2 + X_3)$ and $(X_4 + X_5 + X_6 + X_7)$ as linear functions of C/H weight ratio best fit the data. The following argument is proposed to support the trends exhibited by these correlations.

To assume that the feedstock having a larger aromatics content will also contain a greater amount of aromatics in its initial breakdown is reasonable. The same feedstock will subsequently have less alkanes and alkenes, and a logical assumption to follow is that the initial breakdown will also have a smaller alkane/alkene content. The parameters $(X_1 + X_2 + X_3)$ and $(X_4 + X_5 + X_6 + X_7)$ represent the amount of alkanes/alkenes and aromatics, respectively, in the initial breakdown. The C/H weight ratio is a qualitative indicator of aromatics content, i.e., a larger ratio usually implies more aromatics in the feedstock (refer to Table 2). The parameter $(X_4 + X_5 + X_6 + X_7)$ increases linearly with C/H weight ratio, whereas the opposite trend is observed for $(X_1 + X_2 + X_3)$. Hence, the proposed argument offers physical justification of these trends.

3. Parity Plots

Having developed correlations which will predict the initial breakdown distribution, the next step was to determine how accurately the kinetic model predicts the effluent compositions. By inputting the feedstock's C/H weight ratio and molecular weight into the six correlations, the characteristic initial breakdown for each feedstock could be calculated. The X_7 group (4-ring aromatic compounds) was assumed to be negligible.

The graphical correlations were translated into mathematical expressions (Table 3).

Having determined the initial breakdowns from the correlations, the effluent compositions for the available pilot plant and laboratory runs were calculated, and these predicted values were compared to the actual results (The computer program used to predict the effluent yields is found in Appendix A). Figures 10 through 15 are parity plots of predicted values versus actual results for the effluent groups W_1, W_2, ..., W_6, respectively. For these plots, each feedstock was distinguished by a different plotter symbol. These symbols, along with the number of GRH runs for each feedstock, are found in Table 4.

Comparing the kinetic model's predictions of the effluent yields for the six lumped groups, the methane (W_1) and ethane/ethylene (W_2) product yields are predicted with the most accuracy, and it's these groups which are of prime interest to the process designers. This result is even more significant when one considers that these two groups account for 68-96%, by weight, of the GRH product. The only exception is the lone Synthetic Fuel Oil run. For this run, methane, ethane and ethylene comprise only 23% of the effluent. Perhaps

Table 3. Mathematical Expressions for Initial Breakdown Correlations

$$Y = mX + b$$

Y	m	b
$(X_1 + X_2 + X_3)$	-0.164	1.83
$(X_2 + X_3)$	-0.184	1.72
$(X_1 + X_3)$	-0.127	1.26
$(X_4 + X_5 + X_6 + X_7)$	0.158	-0.77
$X_4/(X_4 + X_5 + X_6 + X_7)$	-0.00258	1.05
$(X_4 + X_5)/(X_4 + X_5 + X_6 + X_7)$	-0.00143	1.08

Table 4. Feedstock Plotter Symbols

Feedstock	No. of Runs	Plotter Symbol
Butane	1	*
LDF 115	5	⧗
LDF 170	9	□
Natural Gas Condensate	1	◇
Kerosene	2	△
No. 2 Fuel Oil	8	E
Diesel Oil	2	8
Topped Kuwait	10	+
Monagas (Run H-30)	1	Y
Monagas	3	X
Tar Sands	8	H
Synthetic Fuel	1	⧖

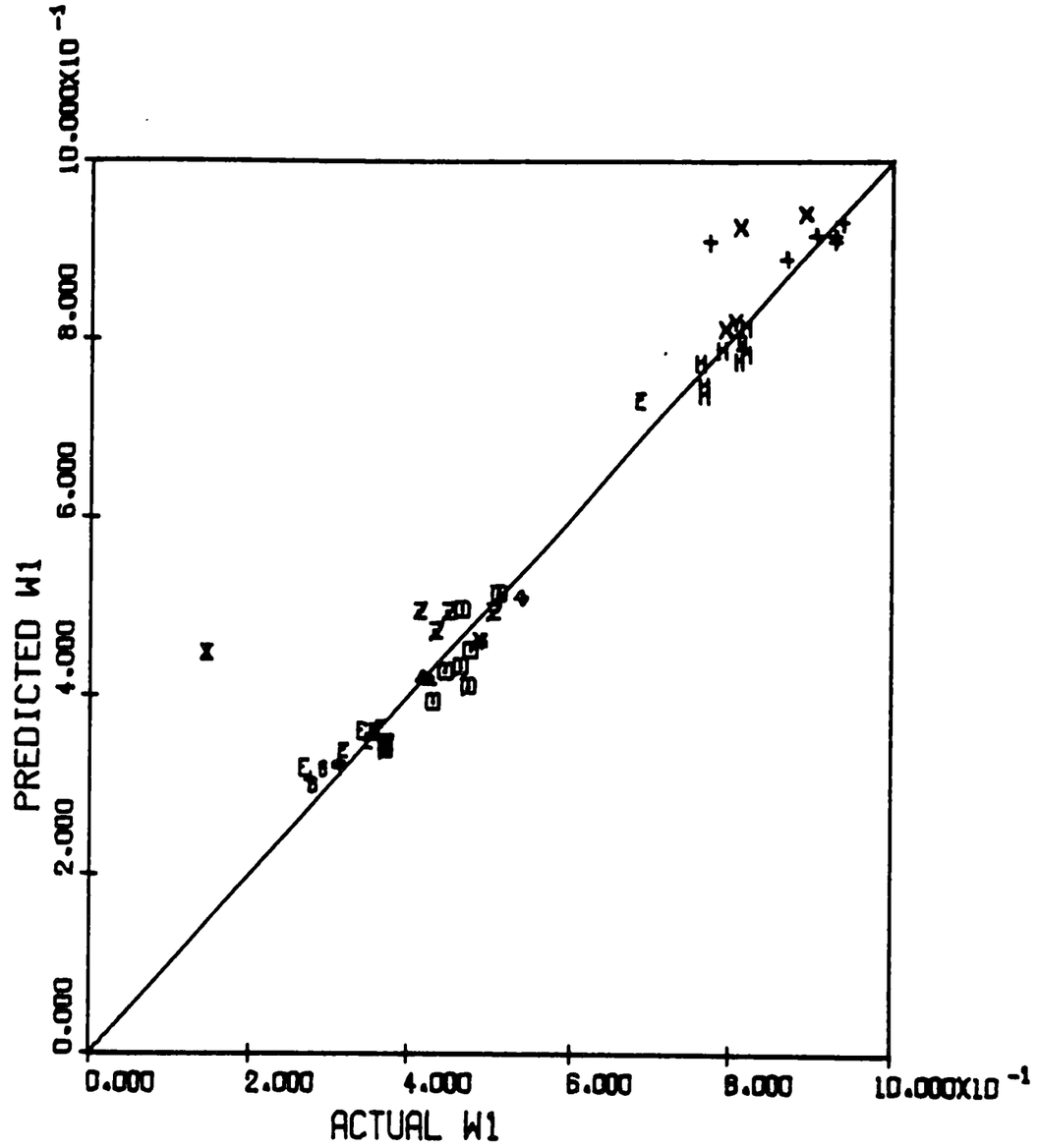

FIGURE 10

W1 (METHANE) PARITY PLOT

Table 4. Feedstock Plotter Symbols

Feedstock	No. of Runs	Plotter Symbol
Butane	1	*
LDF 115	5	Z
LDF 170	9	□
Natural Gas Condensate	1	◇
Kerosene	2	△
No. 2 Fuel Oil	8	E
Diesel Oil	2	8
Topped Kuwait	10	+
Monagas (Run H-30)	1	Y
Monagas	3	X
Tar Sands	8	H
Synthetic Fuel	1	⧖

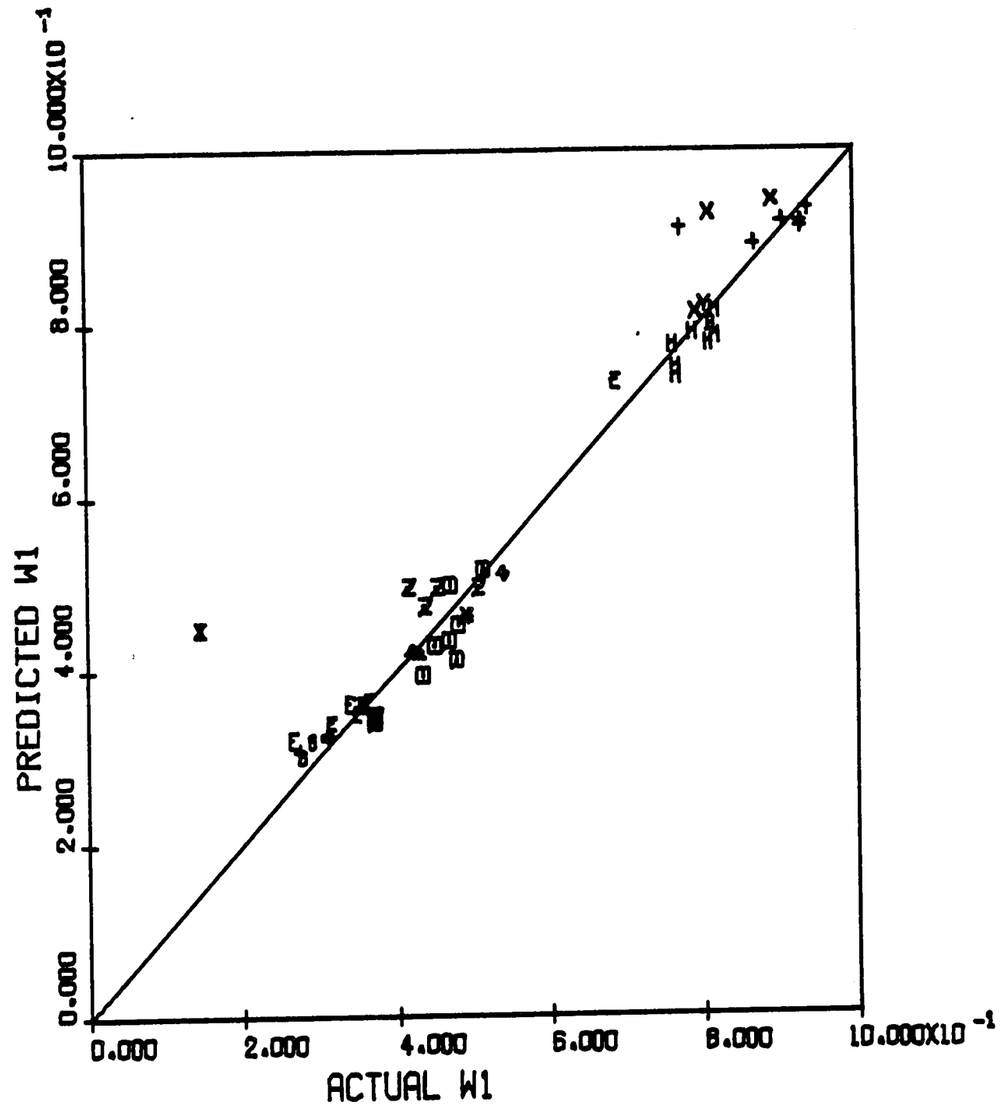

FIGURE 10

W_1 (METHANE) PARITY PLOT

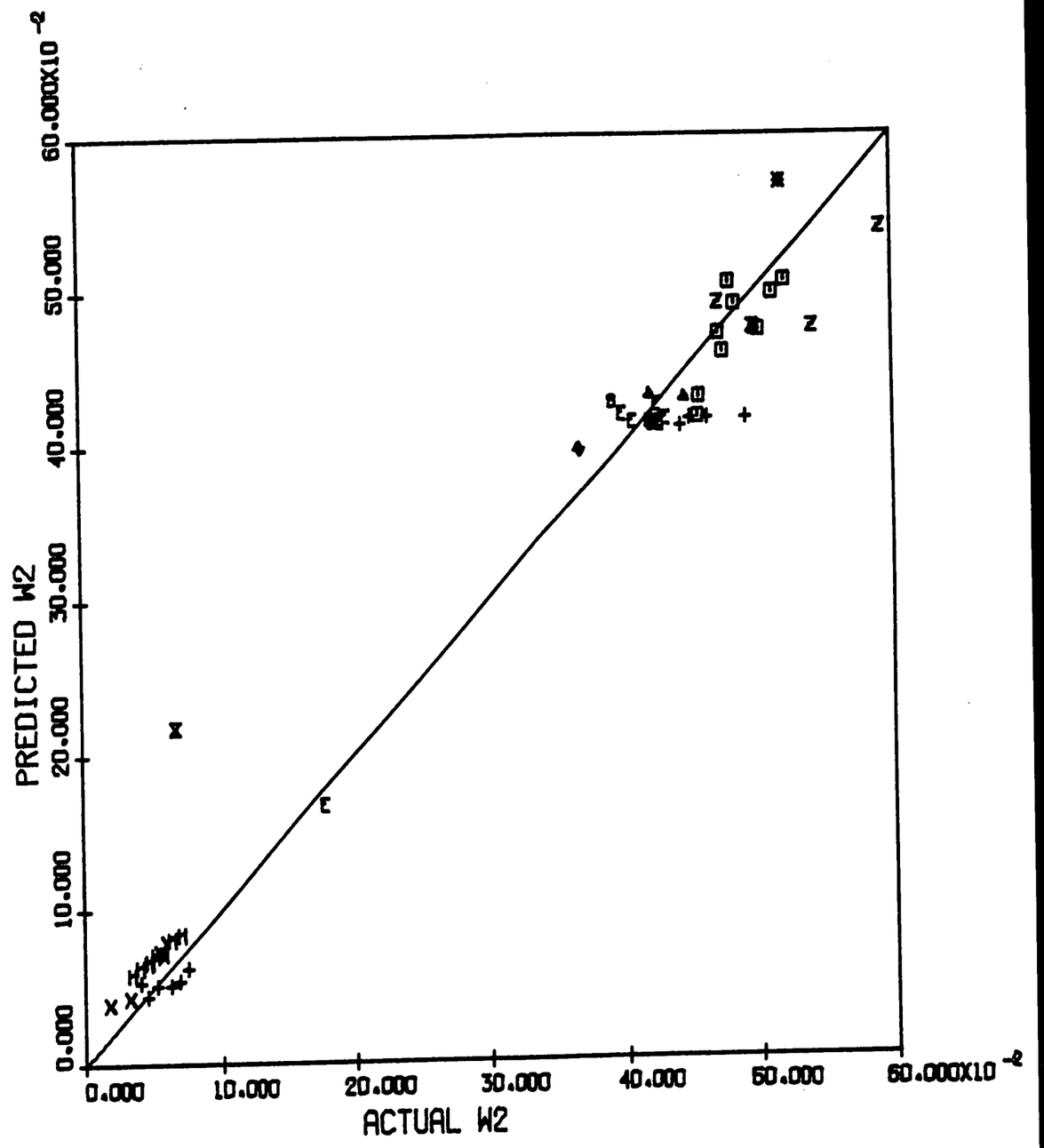

FIGURE 11

W_2 (ETHANE/ETHYLENE) PARITY PLOT

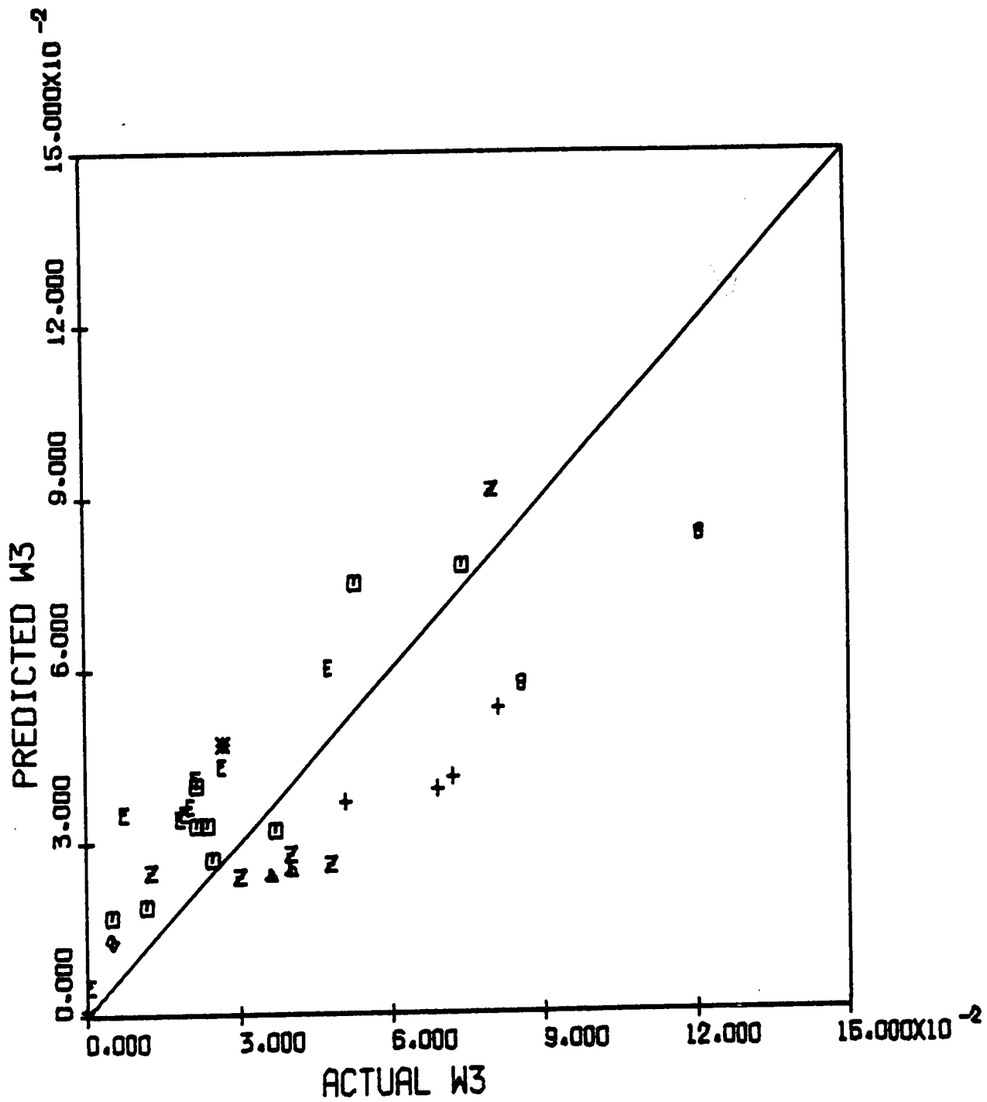

FIGURE 12

W_3 (PROPANE/PROPYLENE +) PARITY PLOT

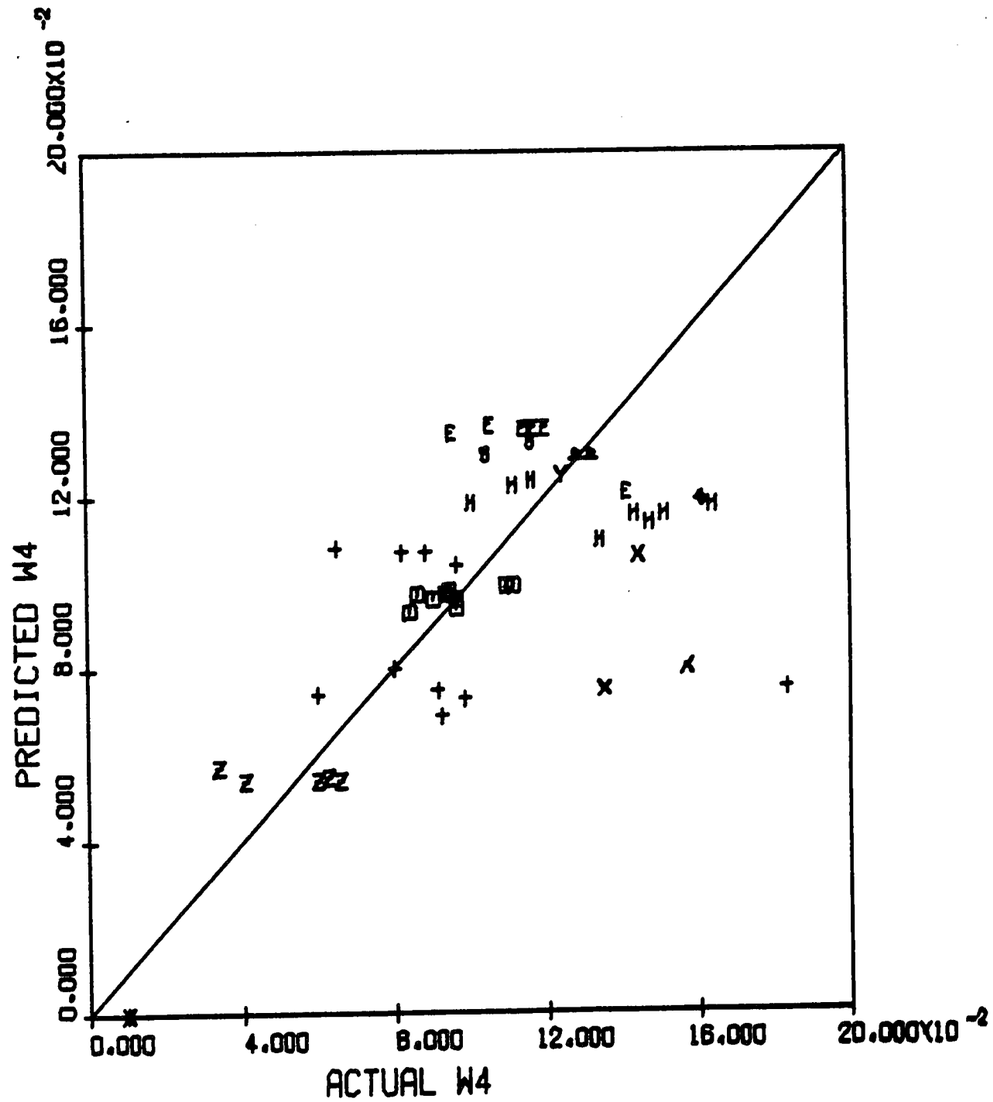

FIGURE 13

W4 (BTX) PARITY PLOT

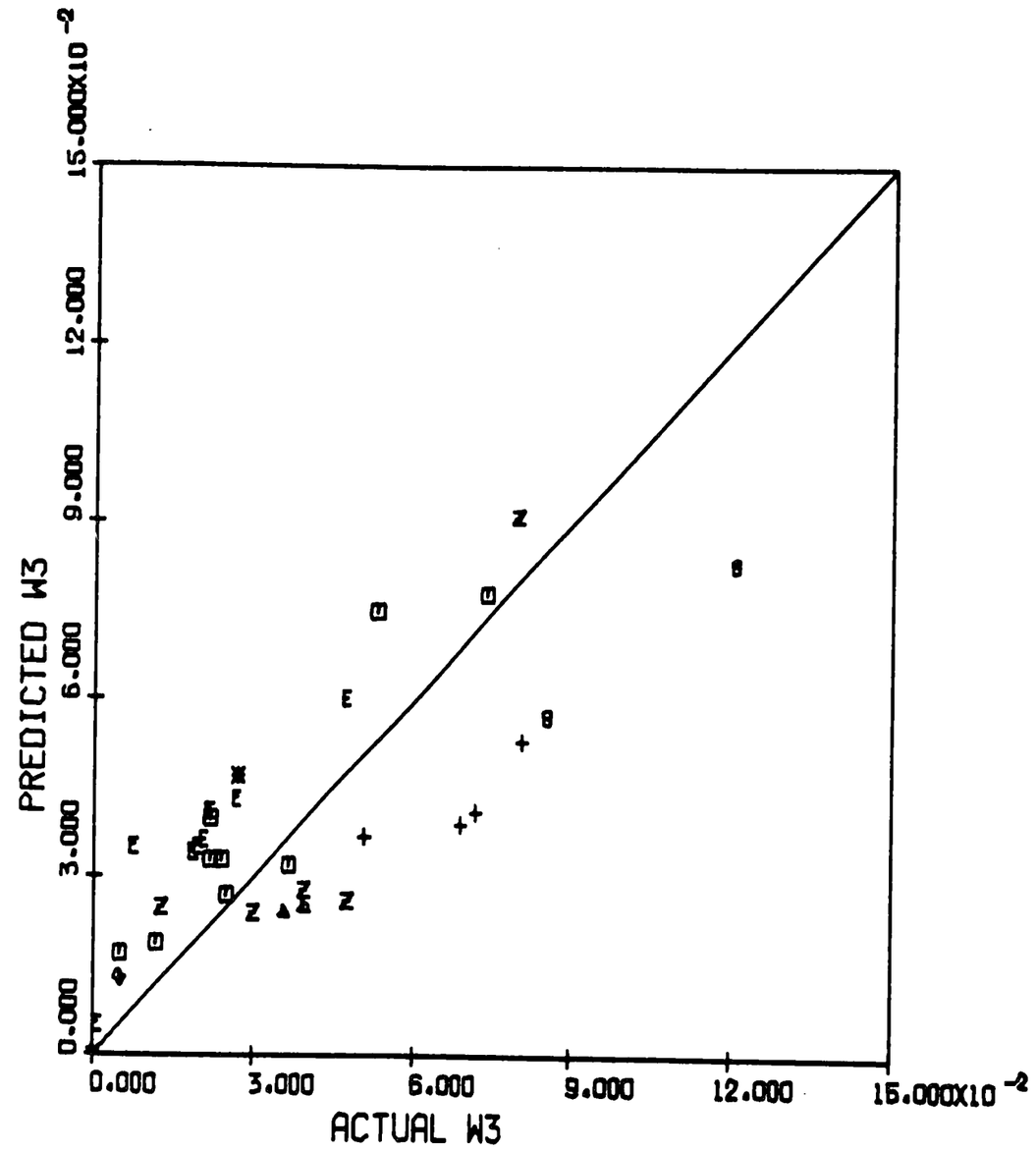

FIGURE 12

W3 (PROPANE/PROPYLENE +) PARITY PLOT

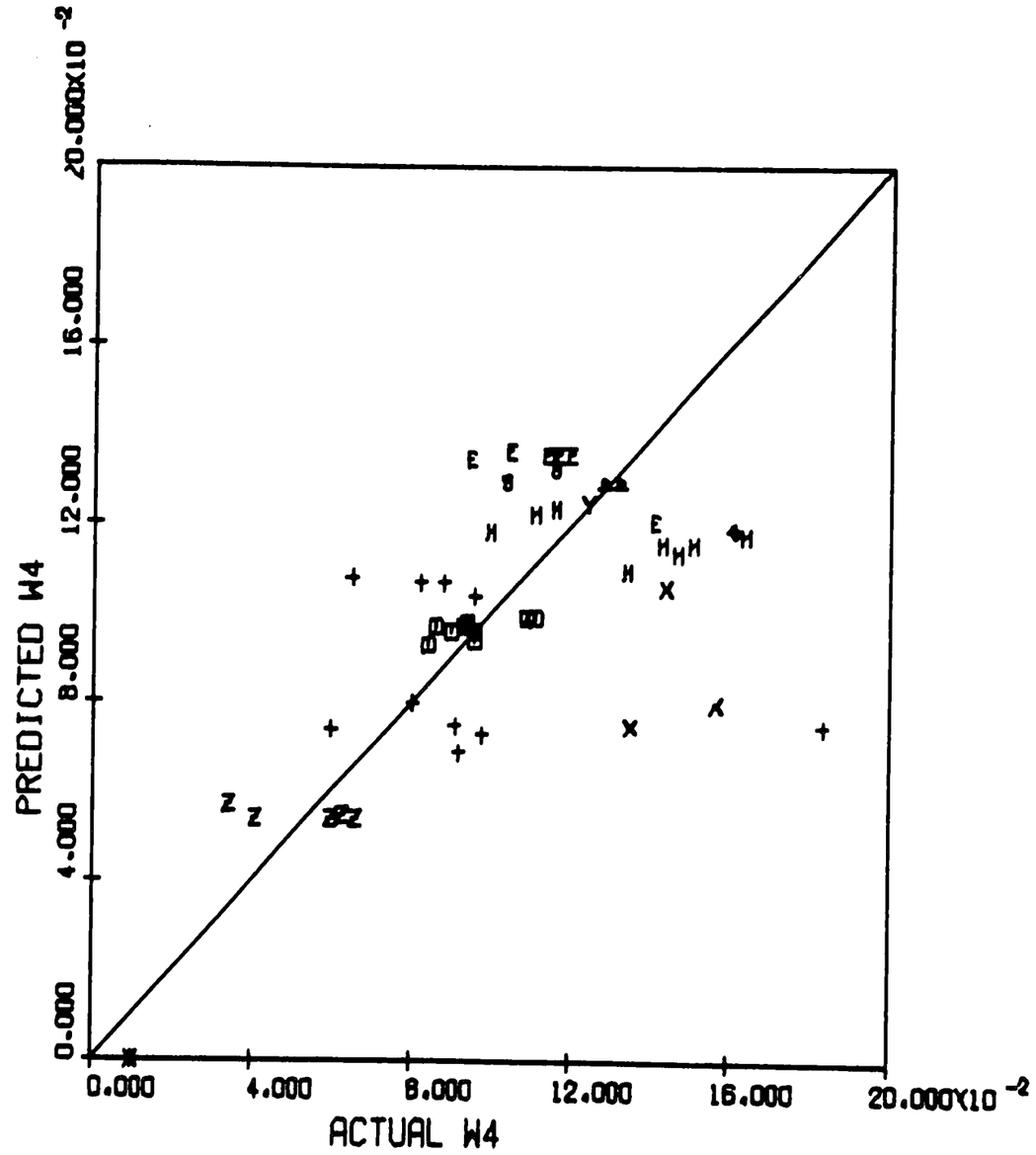

FIGURE 13
W4 (BTX) PARITY PLOT

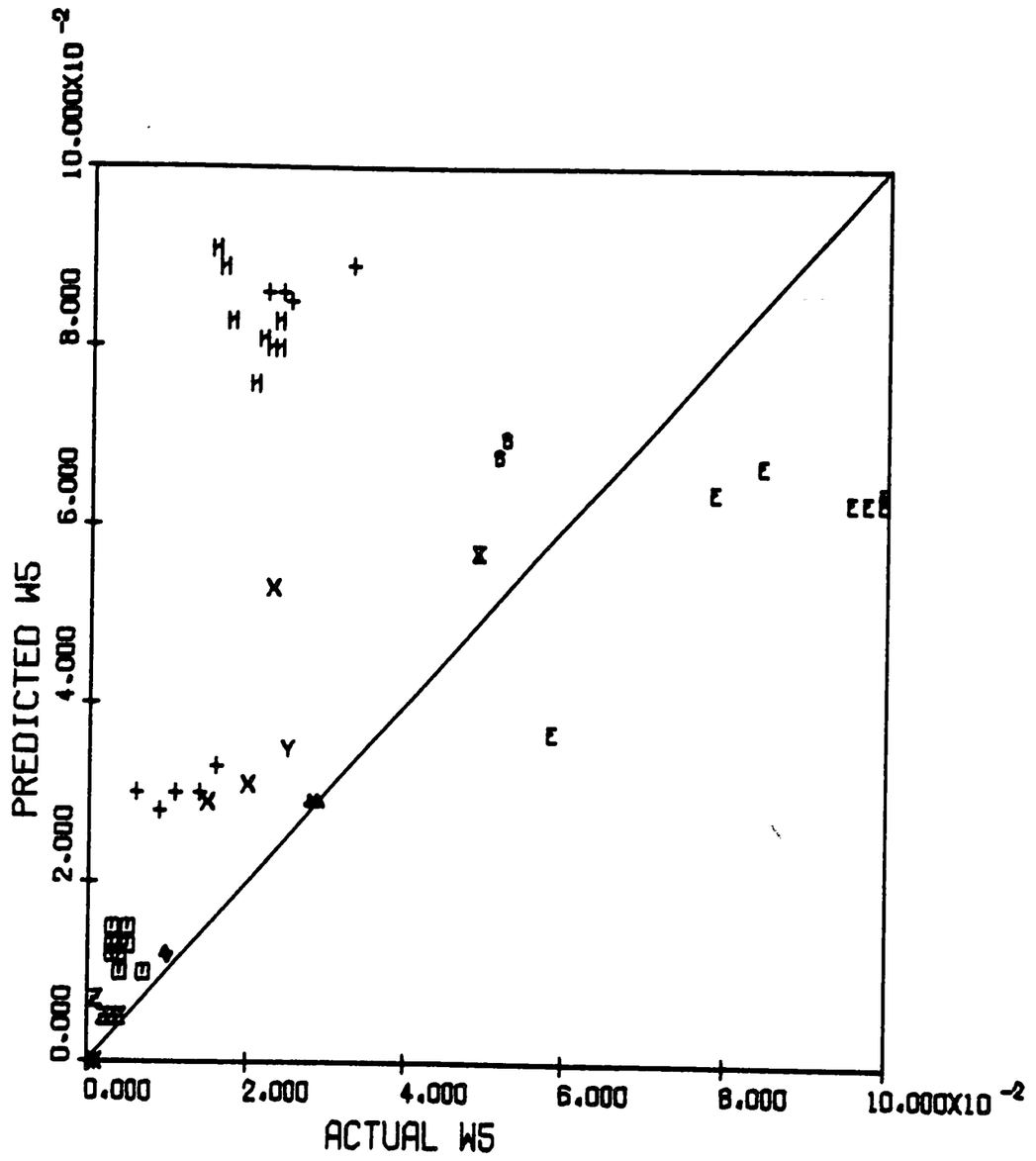

FIGURE 14

W_5 (NAPHTHALENE) PARITY PLOT

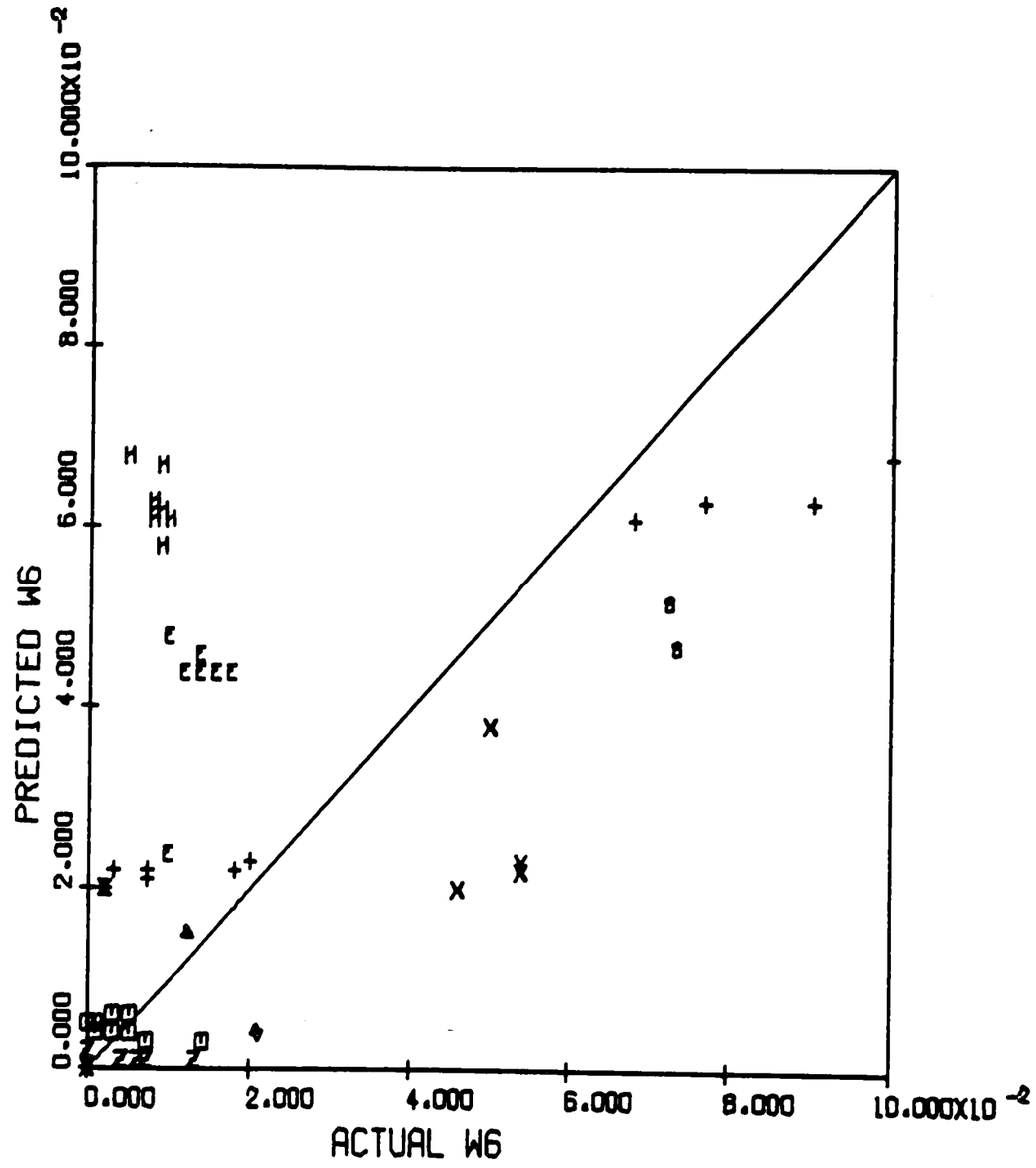

FIGURE 15

W_6 (ANTHRACENE) PARITY PLOT

not so coincidentally, the model's worst prediction for both W_1 and W_2 effluent yields is the Synthetic Fuel Oil run. (See Figures 10 and 11 where the hourglass symbol denotes the Synthetic Fuel Oil feedstock).

In comparison to the W_1 and W_2 parity plots, there is more scatter of the data points relative to the 45 degree line for the W_3 parity plot (Figure 12) which means that the model is less accurate when predicting W_3 effluent yields. On the other hand, a substantial number of runs have not been represented on the W_3 parity plot because of their proximity to the origin. The W_3 yields were zero for six Topped Kuwait runs and all the Monagas, Athabasca Tar Sands and Synthetic Fuel Oil runs. The model has either predicted zero or 0.001 for these runs. These nineteen runs, which were very accurately predicted but not represented on the parity plot, certainly improve the confidence level of the model's ability to predict W_3 yields.

The parity plots for W_4, W_5 and W_6 (Figures 13, 14 and 15, respectively) reveal that the model is weak in predicting the aromatics distribution of the effluent. Relative to the other aromatic groups, the W_4 product yields (benzene, toluene and xylene) were

the largest, and also were predicted with the most accuracy. The kinetic model substantially overpredicted the W_5 effluent yields (2-ring aromatics). Exceptions to this trend were the No. 2 Fuel Oil runs (plotter symbol E) which were underpredicted. Likewise, predictions for the W_6 effluent yields (3-ring aromatics) were too high rather than too low by a 2:1 ratio. The W_6 yields were overpredicted for all the No. 2 Fuel Oil and Athabasca Tar Sands runs (plotter symbol H).

The model's poor predictive capability for the aromatic groups is probably the result of the weak correlations of $X_4/(X_4 + X_5 + X_6 + X_7)$ and $(X_4 + X_5)/(X_4 + X_5 + X_6 + X_7)$ as functions of feedstock molecular weight. However, the aromatics, especially the 2- and 3-ring compounds, account for less than 30% of the product weight in virtually all the GRH runs. Therefore, the absolute error is much less than the relative error for the predicted values of the aromatic yields.

4. Mass Balances

An overall mass balance between the hydrocarbon feed and the effluent is always satisfied because the predicted effluent yields are given in terms of pounds of product per pound of oil fed. Likewise, the hydrogen will always balance because of the excess hydrogen in the GRH (Excess H_2 prevents carbon deposition

in the reactor).

When using the kinetic model to predict effluent yields, the question of whether a carbon balance exists between the feed and the final product need never be considered because the model predicts the component distribution of the GRH effluent in terms of lumped hydrocarbon groups instead of individual compounds.

However, certain uses of the kinetic model such as a process design analysis of a proposed GRH run will require a specification of the individual effluent components. In this case a carbon balance is important and can be effected only by having a correct set of distribution ratios for the specific components in the several effluent groups (For example, the predicted effluent yield for W_2 must be proportioned between ethane and ethylene). The determination of these ratios should be based on experimental data to the extent that such is available.

The GRH kinetic model was used by the Process Engineering Group at Air Products to predict effluent flows for four proposed feedstock runs at Air Products' Marcus Hook Facility [3]. Related experimental data

were available which provided a detailed component analysis of the effluent. These were used to make a first estimate of the component distributions within the hydrocarbon groups [5]. However, the ethane/ethylene split for the W_2 effluent group was allowed to vary in order to achieve a rigorous carbon balance. In all four cases, the adjustments to the ethane/ethylene split were small relative to the split suggested by the experimental data [4].

5. Temperature Effects

In developing the GRH kinetic model, Weimer assumed that the initial breakdown was independent of reactor temperature [21]. In an attempt to refine the model, an investigation was made as to whether temperature may be a parameter in any of the existing correlations involving feedstock properties, or whether temperature might provide, by itself, an additional correlation needed to determine the initial breakdown. Both the temperature at which the feedstock enters the reactor, i.e. the preheat temperature, and the reactor temperature were considered. Since the assumed initial breakdown of the feedstock occurs before the reactants attain reactor temperature, it was hoped that preheat temperature rather

than GRH temperature would provide some type of correlation. However, if the GRH reactor temperature proves to be the correlating parameter, it can be argued that the initial breakdown occurs very, very rapidly in the reactor at reactor temperature, and, thereafter, the kinetics assume control.

A review of the data (Appendix B) revealed no direct correlation of the initial breakdown groups or their correlating groups (e.g., $X_1 + X_2 + X_3$) as a function of GRH preheat temperature. Increasing preheat temperatures did not coincide with either an increasing or decreasing trend in the initial breakdown component yields or their correlating groups.

Having discovered no trend with preheat temperatures, attention was then focused on the effect of reactor temperature on the initial breakdown. Partially-vaporized Topped Kuwait crude oil was the only feedstock for which a substantial number of runs were performed over a wide GRH temperature range. Four runs were performed at reactor temperatures in the 1320-1340°F range and six runs in the 1635-1665°F range (refer to Table B-6). For the high temperature runs, the amount of X_3 (propane, propylene and heavier

paraffins) in the initial breakdown was zero compared to an average of 0.287 pound of X_3 per pound of oil fed for the low temperature runs. The benzene/toluene/xylene group, X_4, seems to increase in quantity with increasing temperature, as shown in Figure 16. In Figure 17, the sum ($X_1 + X_2$) exhibits a more pronounced increase with higher reactor temperatures.

Although preheat temperature effects can be discounted, additional data aimed at isolating the reactor temperature effects on the initial breakdowns of various feedstocks are required before a conclusion can be drawn. Consequently, the correlations (Figures 16 and 17) developed from the Topped Kuwait feedstock runs were not used to determine initial breakdown distributions.

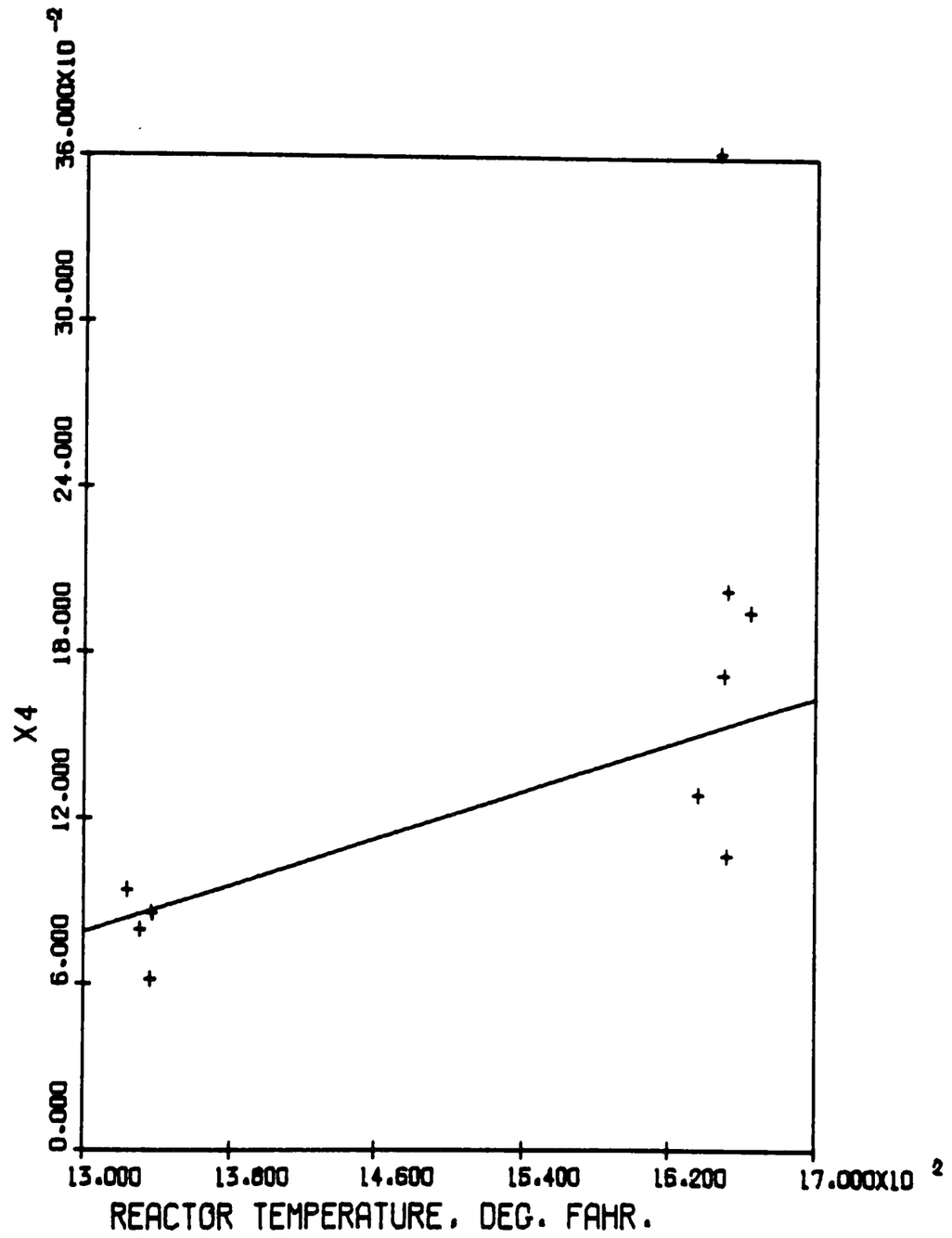

FIGURE 16

INITIAL BREAKDOWN TEMPERATURE EFFECTS

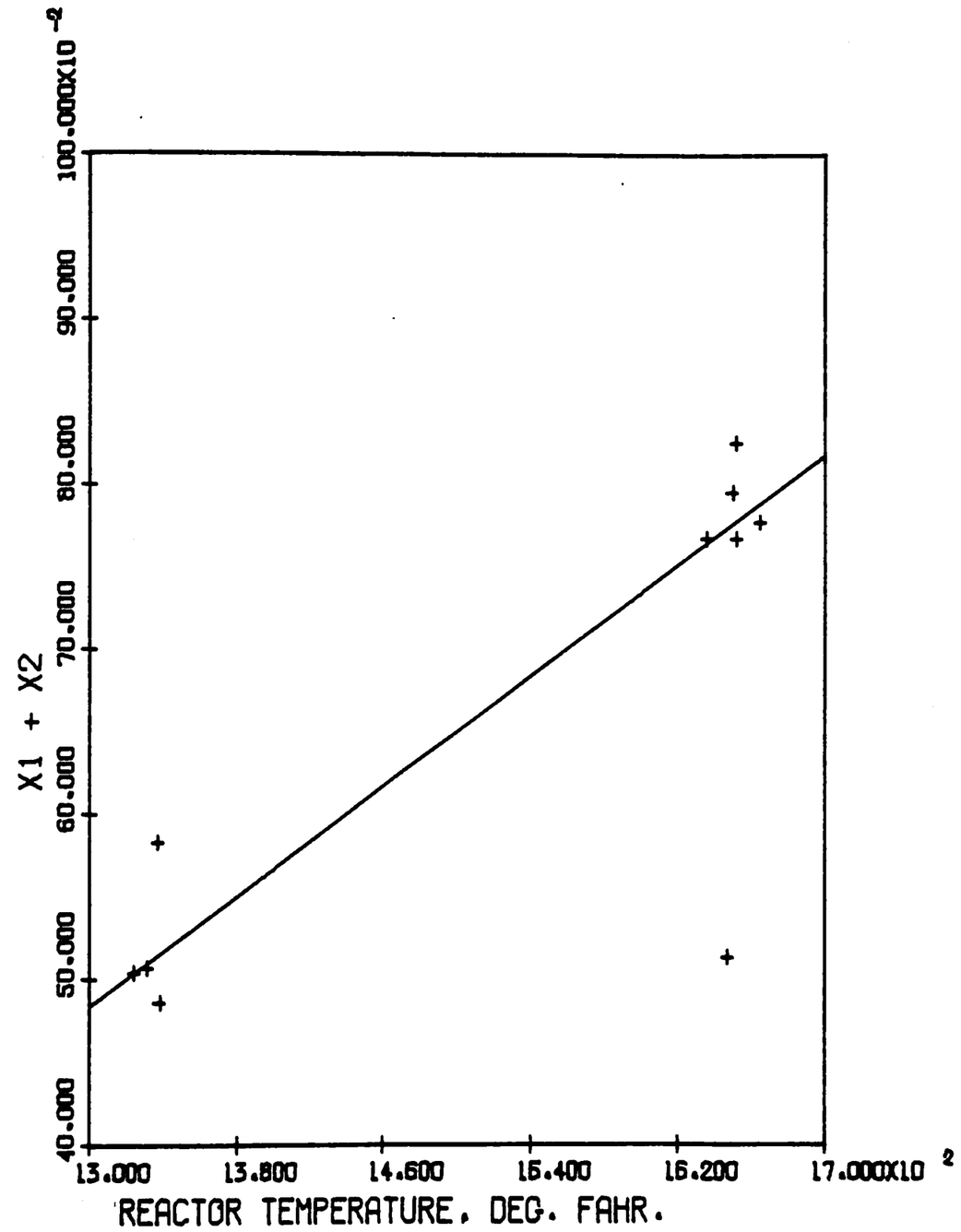

FIGURE 17

INITIAL BREAKDOWN TEMPERATURE EFFECTS

D. Summary

The GRH kinetic model originally proposed by Weimer has been extended by considering an enlarged data base and by the development of correlations (Figure 4-9) that determine the initial breakdown as a function of characteristics of a particular feedstock. Given the residence time and reactor temperature, the prediction of GRH effluent yields is possible once the initial breakdown has been determined. The predictive accuracy of the extended model has been tested by calculating effluent yields for fifty-one GRH runs and comparing these results to actual values.

On the average, the kinetic model predicted the methane and ethane/ethylene yields to within ±5 and 16%, respectively, of their actual values. Although able to predict the total aromatic content of the effluent to within ±26% (average) of the observed results, the model was very weak in predicting (W_5) and anthracene (W_6) groups. Two possible explanations can be offered. First, the accuracy of the actual values for aromatic yields is questionable. For many runs, the 3- and 4-ring aromatic compounds were lumped together in the effluent-yield analysis. In these cases, it was assumed that the amount of 4-ring aromatic compounds was negligible. Secondly, and probably more important, two of the correlations (Figures 8 and 9) developed to

determine the quantity of aromatics in the initial breakdown were poor fits of the data.

When one considers that methane, ethane and ethylene comprise at least 70% of the product weight, the model's inability to predict accurately the aromatic effluent yields is overshadowed by its accurate predictions of the methane and ethane/ethylene effluent yields. The simplicity of the model and the diversity of the feedstocks considered make these results even more encouraging. The true test of this kinetic model will be how well it can incorporate new feedstocks and future data.

determine the quantity of aromatics in the initial breakdown were poor fits of the data.

When one considers that methane, ethane and ethylene comprise at least 70% of the product weight, the model's inability to predict accurately the aromatic effluent yields is overshadowed by its accurate predictions of the methane and ethane/ethylene effluent yields. The simplicity of the model and the diversity of the feedstocks considered make these results even more encouraging. The true test of this kinetic model will be how well it can incorporate new feedstocks and future data.

E. Recommendations

1. From the limited data available, it has been demonstrated that the initial breakdown parameters X_4 and $(X_1 + X_2)$ are increasing functions of reactor temperatures. Future laboratory or pilot plant GRH studies should be aimed at isolating the effect of reactor temperature on initial breakdown for various feedstocks. The possibility of these parameters serving as a basis for improved correlations could then be investigated.
2. Future GRH runs should include a detailed analysis of the effluent components. Specifically, the polycyclic aromatics should be reported with more resolution relative to 2-, 3- and 4-ring compounds. Perhaps then a correlation to predict X_7 could be developed.
3. The effect of other reactor operating conditions, such as reactor pressure and the volume ratio of hydrogenating gas to distillate feed, on initial breakdown could be investigated.
4. After the above issues have been resolved, the kinetic rate constants should be fine tuned to improve the model's predictive powers. Relative to Weimer's proposed values, the rate constants have already been adjusted using a trial-and-error technique. However, a numerical analysis method should be used for future adjustments.

IV. FIRST-PRINCIPLES APPROACH

A. Introduction

Prior to pursuing Weimer's original kinetic model, an alternate modeling approach was considered. The chief difference between approaches was that the reactants in Weimer's reaction scheme consisted of groups of similar compounds formed from an assumed initial breakdown of the feedstock, whereas this alternate approach regarded the reaction species to be the specific chemical compounds which comprise the feedstock. In reference to this fundamental difference, the alternate modeling effort was dubbed the "First-Principles Approach". The obvious advantage of this type of kinetic model over the Weimer model is the ability to predict the effluent yields of individual species rather than lumped groups.

A goal was set to develop a kinetic model, via the First-Principles Approach, with the ability to predict GRH effluent yields for an LDF 170 feedstock (light distillate fraction with a boiling end point of 170°C). A linearly independent set of chemical reactions was desired that would accurately represent the dynamic behavior of the highly coupled system of chemical reactions occurring within the GRH. The reaction scheme was to be developed using only first order reactions. An analogy can be made

between the role of a first order system in the chemical kinetics of complex systems and that of the equation of state for an ideal gas in classical thermodynamics [20]. The first order system is an idealized representation of the rate processes.

Instead of initially attempting to develop a kinetic model for LDF 170, a building-block approach was employed. Simple reaction schemes and the appropriate rate constants were to be developed successively for the thermal hydrocracking of pure ethane, propane, n-butane and finally LDF 170. Each case was to be an extension of the reaction scheme for the previous feedstock. As an example, the extension of the ethane hydrocracking kinetic model to include propane hydrogenolysis required the addition of chemical reactions to the model which would account for the additional products introduced by the heavier feedstock (propane). However, the kinetic rate constants developed previously for the chemical reactions describing ethane hydrogenolysis were not to be changed. Only the rate constants for the additional reactions needed to be determined. In this manner, progression to heavier feedstocks should occur until a kinetic model was developed that would predict the effluent yields for LDF 170 GRH runs.

B. Numerical Analysis Methods

Each kinetic model consisted of a chemical reaction scheme whose kinetics were expressed as first-order rate equations. For practical convenience when reducing the data, the rate equations were written in terms of partial pressure which in turn was expressed as the product of the mole fraction and the total pressure. The introduction of mole fractions into the rate expressions resulted in a kinetic model consisting of nonlinear differential equations -- the unknowns being the kinetic rate constants.

Published effluent yield data [17] for ethane, propane and n-butane hydrogenolysis have been studied in an effort to determine the rate constants. Numerical support of this work was kindly provided by Dr. Ken Anselmo of the Management Information Department at Air Products and Chemicals, Inc. The numerical methods involved a nonlinear least squares routine coupled with a routine to integrate the model's rate equations. The former routine employs a finite difference Levenberg-Marquardt approach [7] to determine rate constants which will provide accurate predictions of the effluent yields. The integration routine [8] uses collocation methods known to be particularly effective in solving stiff ordinary differential equations. Originally, a standard Runge-Kutta method was used, but extraordinarily small step sizes were

required which indicated the possibility of stiff equations [1].

The numerical routine to determine the kinetic rate constants is an iterative procedure. Input data consist of component feed rates, actual effluent yields and initial estimates of the rate constants. The feed rates are the initial conditions for a set of ordinary differential equations (o.d.e.'s) which make up the kinetic model. The o.d.e.'s are integrated over the entire reactor volume to determine effluent yields. The nonlinear least-squares routine compares these integrated values with actual results and adjusts the rate constants to achieve better agreement. The above procedure of integration, comparison and adjustment is then repeated until the rate constants are no longer changed by the least squares routine.

C. Kinetic Models for the Hydrogenolysis of Paraffins

1. Literature Data

In an attempt to develop kinetic models for ethane, propane and n-butane hydrogenolysis, the effluent yield data were obtained from published literature. Schultz [17] studied the kinetics of the thermal hydrogenolysis of these low-molecular-weight paraffins in a flow system at 1000 psig and 1000 to 1200°F. The hydrogen flow rate satisfied the stoichiometric feed ratio needed for complete hydrocarbon conversion to methane. The flow system was a tubular reactor with an inside sleeve of stainless steel construction. The inside sleeve was two inches in diameter and 35 inches long which produced an overall reactor volume of 0.0636 cubic feet.

2. Ethane Hydrogenolysis

Schultz postulated a free radical mechanism to interpret the results of his ethane hydrogenolysis studies [17]. He found that the predicted rate for the initiation reaction, $C_2H_6 \longrightarrow 2CH_3$, agreed closely with the observed rate of ethane disappearance. Schultz also concluded that the product distribution of ethane hydrocracking could be reasonably represented by the simple model:

$$C_2H_6 + H_2 \xrightarrow{K_1} 2CH_4$$

A review of the data revealed that over 98 mole percent of the effluent consisted of ethane, hydrogen and methane. Inerts (N_2, CO_2 and CO), ethylene and heavier olefins, and heavier paraffins made up the remainder. The inerts were probably introduced into the reaction system with the commercial-grade cylinder hydrogen. Therefore, the proposed kinetic model accounted for virtually all of the effluent components.

Using the numerical analysis techniques previously discussed, the kinetic rate constants were determined, and the effluent yields predicted from the following first-order rate expressions:

$$\frac{-d[C_2H_6]}{dV} = \frac{-d[H_2]}{dV} = \frac{1}{2}\frac{d[CH_4]}{dV} = K_1 \cdot X(C_2H_6) \cdot P_T$$

where the rates of formation (disappearance) are in lb-moles per hour per cubic foot of reactor volume, $[C_2H_6]$ is the molal rate of flow (lb moles/hr) of C_2H_6 into the volume element, dV, $X(C_2H_6)$ is the mole fraction of ethane, P_T is the total pressure in atmospheres and K_1 is the kinetic rate constant in appropriate units.

Ten ethane hydrogenolysis runs performed by Shultz were simulated. The kinetic rate constants were determined and the resultant predictions of the effluent

yields for each run are listed in Table 5. The objective of the numerical analysis routines was to converge on a kinetic rate constant which would provide the most accurate effluent yield predictions. Therefore, it was not surprising to observe such good agreement between the actual and predicted values.

The Arrhenius relationship for the ethane hydrogenolysis rate constant, K_1', was determined from a least squares fit of the data in the form of ln K_1 versus 1/T (Figure 18), where T is in absolute temperature (°R). The resulting expression is:

$$K_1 = 7.26 \times 10^8 \exp(-95{,}674/RT)$$

where the rate constant is in terms of lb-mole/hr/ft^3/psia, T is in °R and R is the universal gas constant, 1.987 Btu/°R/lb-mole. An indication of the quality of fit achieved by the linear regression is the statistical quantity termed the coefficient of determination. For this regression analysis, the coefficient was 0.89. Values close to 1.00 indicate a good fit.

Table 5. Ethane Hydrogenolysis [17]

Pressure: 1000 psig Reactor Volume: 0.0636 cu. ft.

Run No.	C	G	B	D	F	H	I	K	L	M
Reactor Temp., °F	1130	1215	1080	1125	1160	1210	1070	1115	1150	1210
Feed Rates, lb-mole/hr										
Ethane	0.0223	0.0228	0.0436	0.0438	0.0435	0.0439	0.0875	0.0872	0.0878	0.0859
Hydrogen	0.0197	0.0201	0.0384	0.0386	0.0384	0.0387	0.0769	0.0767	0.0722	0.0756
Total	0.0420	0.0429	0.0820	0.0824	0.0819	0.0826	0.1644	0.1639	0.1600	0.1615
Effluent Flow Rate, lb-mole/hr	0.0412	0.0433	0.0825	0.0837	0.0842	0.0839	0.1631	0.1664	0.1590	0.1651
Effluent Compositions: lb-mole/hr										
C_2H_6, actual	0.0205	0.0172	0.0434	0.0436	0.0417	0.0369	0.0871	0.0900	0.0837	0.0801
C_2H_6, predicted	0.0215	0.0169	0.0429	0.0428	0.0403	0.0363	0.0867	0.0858	0.0848	0.0757
H_2, actual	0.0190	0.0142	0.0377	0.0380	0.0360	0.0317	0.0744	0.0735	0.0693	0.0645
H_2, predicted	0.0189	0.0142	0.0377	0.0376	0.0352	0.0311	0.0761	0.0753	0.0742	0.0654
CH_4, actual	0.00166	0.0119	0.0014	0.0021	0.0065	0.0153	0.0016	0.00284	0.00607	0.0204
CH_4, predicted	0.00166	0.0118	0.0014	0.0021	0.0065	0.0152	0.0016	0.00284	0.00609	0.0203
$K_1 \times 10^5$ lb-mole/hr/psia/ft^3	2.47	19.9	2.06	3.10	9.80	24.3	2.34	4.17	9.03	31.5

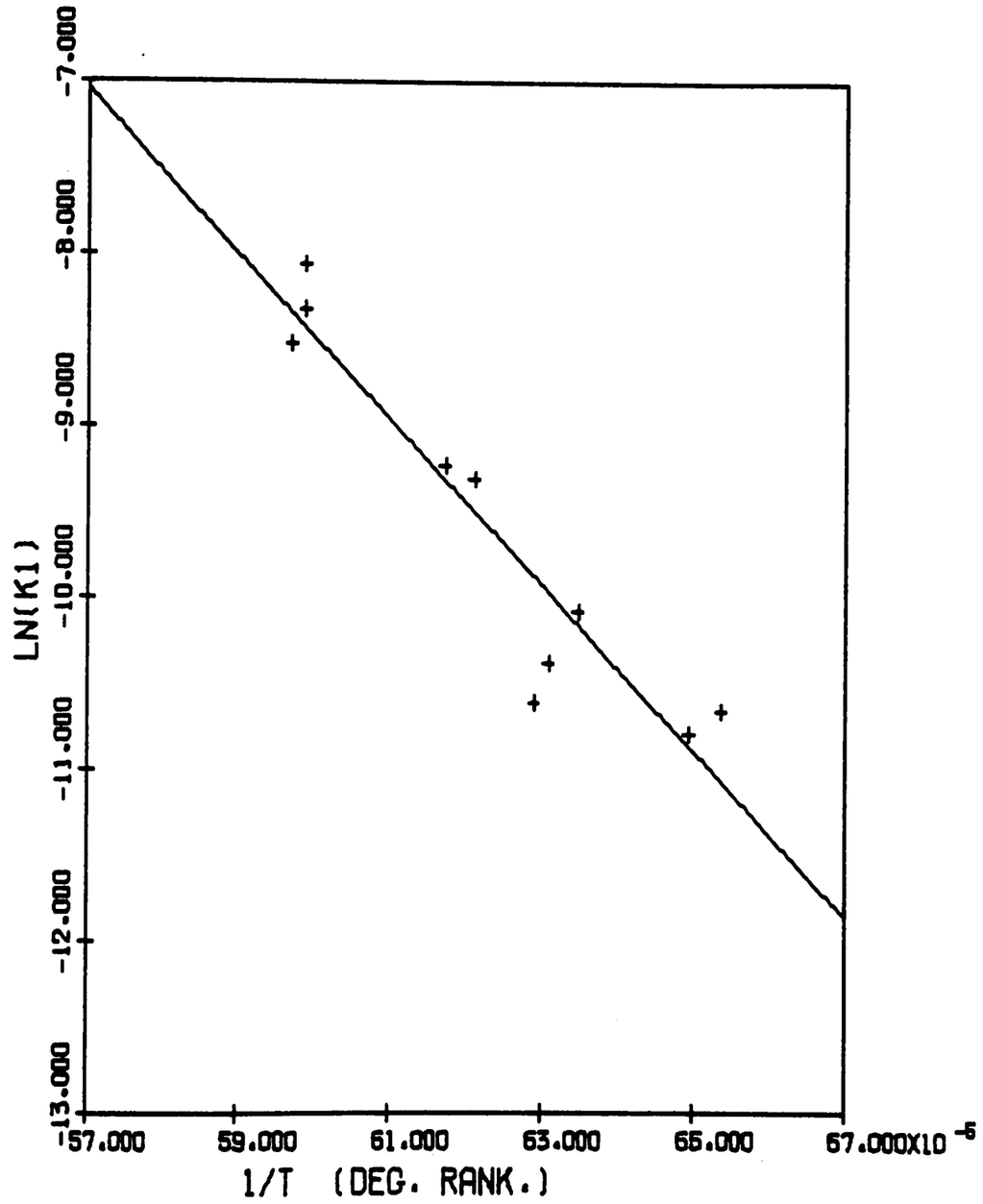

FIGURE 18

LEAST SQUARES FIT OF ETHANE HYDROGENOLYSIS RATE CONSTANT (K_1)

3. Propane Hydrogenolysis

From his studies, Shultz concluded that the product distribution of propane hydrogenolysis could be represented closely by the following model:

$$C_3H_8 + H_2 \xrightarrow{K_2} C_2H_6 + CH_4$$

$$C_2H_6 + H_2 \xrightarrow{K_1} 2CH_4$$

The proposed model accounted for almost all of the effluent from the propane hydrogenolysis runs. Less than one mole percent of the product consisted of compounds unaccounted for by the model: higher paraffins, ethylene, propylene, butylenes and acetylene.

The rate constant, K_1, that had been calculated for the pure ethane runs was used as the rate constant for the overall disappearance of ethane during propane hydrogenolysis. The kinetic rate constant, K_2, and the effluent yields were computed based on the following rate equations:

$$\frac{d[C_3H_8]}{dV} = -K_2 \cdot X(C_3H_8) \cdot P_T$$

$$\frac{d[C_2H_6]}{dV} = K_2 \cdot X(C_3H_8) \cdot P_T - K_1 \cdot X(C_2H_6) \cdot P_T$$

$$\frac{d[CH_4]}{dV} = 2 \cdot K_1 \cdot X(C_2H_6) \cdot P_T + K_2 \cdot X(C_3H_8) \cdot P_T$$

$$\frac{d[H_2]}{dV} = -K_2 \cdot X(C_3H_8) \cdot P_T - K_1 \cdot X(C_2H_6) \cdot P_T$$

Shultz performed eleven propane hydrogenolysis runs. Based on the rigorousness of their carbon balances, seven of these runs were chosen to be simulated. For each of the runs, the kinetic rate constant, K_2, which best predicted the effluent yields was determined. These results are listed in Table 6. With the exception of hydrogen, the propane model predicted the yields with as much accuracy as the ethane model predicted its yields. The hydrogen effluent composition was underpredicted from 1 to 24% in six of the runs and overpredicted by 10% in the remaining run.

A rate constant, K_2, was calculated for each run and an Arrhenius expression was developed via a least squares fit (Figure 19):

$$K_2 = 6.90 \times 10^7 \exp(-76{,}300/RT)$$

where K_2 is in lb-moles/hr/psia/ft^3. The coefficient of determination for the linear regression analysis was 0.93.

4. Effects of Hydrogen Partial Pressure

By expressing the kinetic rate constants in the form of an Arrhenius equation, the only variable which

Table 6. Propane Hydrogenolysis [17]

Pressure: 1000 psig				Reactor Volume: 0.0636 cu. ft.			
Run No.	10	9	2	3	4	5	6
Reactor Temp., °F	945	1045	960	1135	1235	930	1010
Feed Rates, lb-mole/hr							
Propane	0.01472	0.01530	0.0277	0.0276	0.0281	0.0556	0.0565
Hydrogen	0.0282	0.0279	0.0658	0.0550	0.0551	0.1112	0.1127
Total	0.0429	0.0432	0.0935	0.0826	0.0832	0.1668	0.1692
Effluent Flow Rate, lb-mole/hr	0.0461	0.0489	0.0886	0.0874	0.0888	0.1727	0.1707
Effluent Compositions: lb-mole/hr							
C_2H_6, actual	0.00144	0.00893	0.00134	0.0244	0.0216	0.00121	0.0129
C_2H_6, predicted	0.00139	0.00934	0.00148	0.0250	0.0227	0.00138	0.0141
H_2, actual	0.0301	0.0241	0.0587	0.0324	0.0263	0.1150	0.0997
H_2, predicted	0.0268	0.0184	0.0643	0.0284	0.0221	0.1098	0.0986
CH_4, actual	0.00135	0.0102	0.00169	0.0289	0.0406	0.00173	0.0159
CH_4, predicted	0.00139	0.0096	0.00148	0.0274	0.0381	0.00138	0.0141
C_3H_8, actual	0.0132	0.00560	0.0268	0.00175	0.00027	0.0548	0.0422
C_3H_8, predicted	0.0133	0.00588	0.0262	0.00176	0.00027	0.0542	0.0424
$K_2 \times 10^5$ lb-mole/hr/psia/ft^3	6.59	64.0	7.93	352	600	6.94	75.2

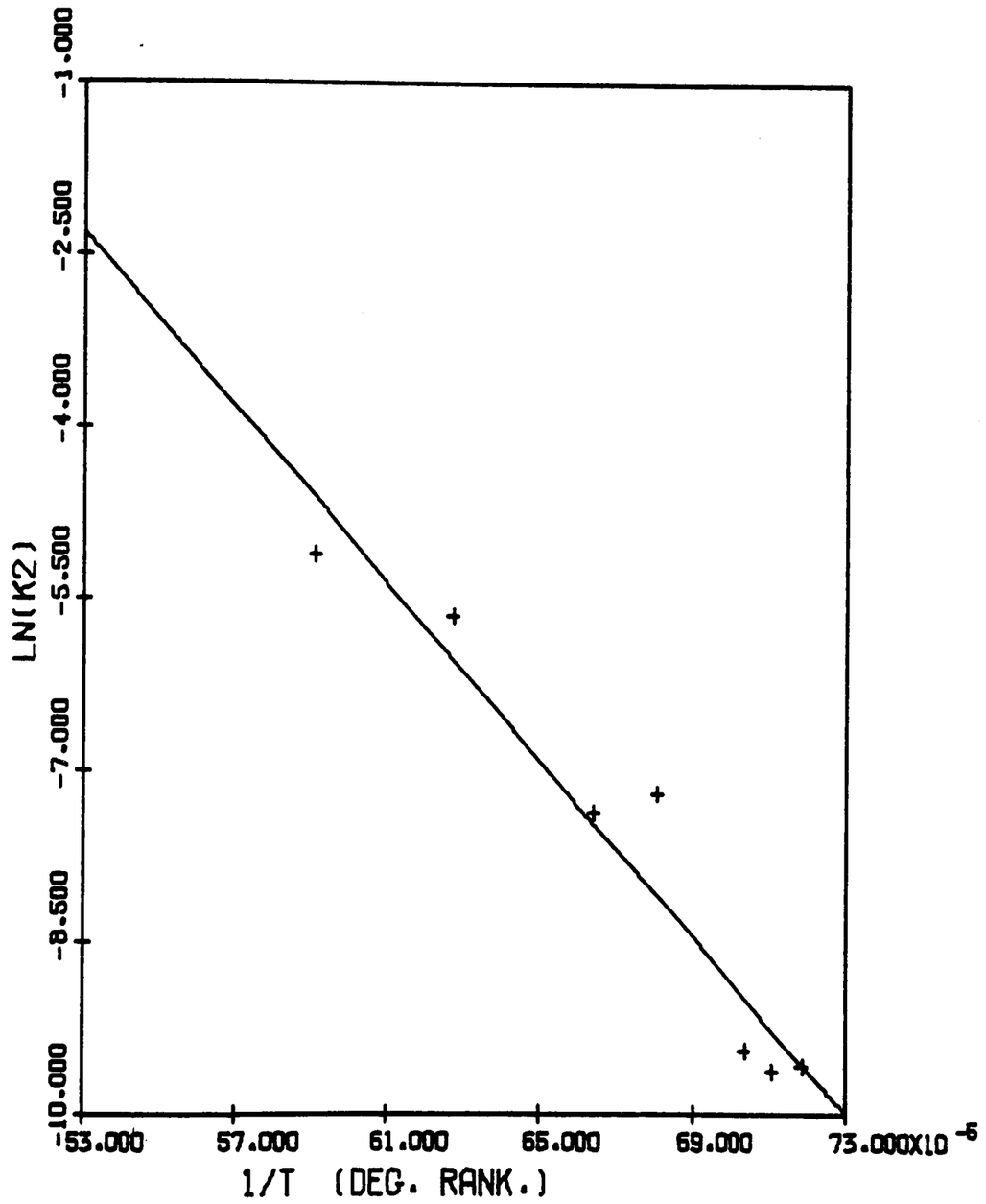

FIGURE 19

LEAST SQUARES FIT OF PROPANE HYDROGENOLYSIS RATE CONSTANT (K_2)

will have a direct effect on the rate constants is temperature. Shultz isolated the effects of pressure by performing three propane hydrogenolysis runs at total pressures of 500, 1000 and 1500 psig while maintaining a constant reactor temperature of 1035°F and a feed ratio of approximately 2 moles H_2/mole C_3H_8. From the results presented in Table 7, it is clear that increased hydrogen partial pressure accelerates the disappearance of propane. The proposed kinetic model for propane hydrogenolysis consists of first-order rate equations which do not explicitly account for the effect of hydrogen partial pressure. Will a second-order mechanism explain the kinetic data better than the proposed first-order model?

To answer this question, the ten runs for pure ethane hydrogenolysis were resimulated using the same reaction scheme. However, the rate equations were written as second-order expressions to include the effect of varying hydrogen partial pressures. The resultant Arrhenius expression is:

$$K_1' = 9.80 \times 10^7 \exp(-100{,}216/RT)$$

where the units of K_1' are lb-moles/hr/psia/ft^3 and the superscript (') indicates that the rate constant is from a second-order rate equation.

The three propane runs at the different pressures were then simulated using both first- and second-order rate expressions. These two cases are depicted in Figure 20. The rate constants, K_1 and K_1', whose Arrhenius expressions were determined from the pure ethane hydrocracking runs were used as the rate constants for the overall disappearance of ethane during propane hydrogenolysis. Therefore, the numerical routines only determined the kinetic rate constants, K_2 and K_2', of the reaction $C_3H_8 + H_2 \rightarrow C_2H_6 + CH_4$ for both the first- and second-order cases, respectively. Table 7 lists the rate constants that were determined and the effluent yields which were predicted. Surprisingly, both mechanisms predicted the same effluent yields. However, the K_2' values show a definite trend with pressure, and therefore the second-order mechanism does not satisfactorily explain the kinetic data. The K_2 values are not only more nearly identical, but the slight variations show no definite trend. Therefore, the assumption of a first-order mechanism seems justified, and this assumption was extrapolated to the kinetic models that follow.

5. n-Butane Hydrogenolysis

The kinetic model which most accurately predicted the product distributions for the n-butane hydrogenolysis

Propane Hydrogenolysis Reaction Scheme

$$C_3H_8 + H_2 \xrightarrow{K_2} C_2H_6 + CH_4$$

$$C_2H_6 + H_2 \xrightarrow{K_1} 2CH_4$$

1st order mechanism:

$$\frac{d[C_3H_8]}{dV} = -K_2 \cdot X(C_3H_8) \cdot P_T$$

$$\frac{d[C_2H_6]}{dV} = K_2 \cdot X(C_3H_8) \cdot P_T - K_1 \cdot X(C_2H_6) \cdot P_T$$

$$\frac{d[CH_4]}{dV} = K_2 \cdot X(C_3H_8) \cdot P_T + 2 \cdot K_1 \cdot X(C_2H_6) \cdot P_T$$

$$\frac{d[H_2]}{dV} = -K_2 \cdot X(C_3H_8) \cdot P_T - K_1 \cdot X(C_2H_6) \cdot P_T$$

2nd order mechanism:

$$\frac{d[C_3H_8]}{dV} = -K_2' \cdot X(C_3H_8) \cdot X(H_2) \cdot P_T^2$$

$$\frac{d[C_2H_6]}{dV} = K_2' \cdot X(C_3H_8) \cdot X(H_2) \cdot P_T^2 - K_1' \cdot X(C_2H_6) \cdot X(H_2) \cdot P_T^2$$

$$\frac{d[CH_4]}{dV} = K_2' \cdot X(C_3H_8) \cdot X(H_2) \cdot P_T^2 + 2 \cdot K_1' \cdot X(C_2H_6) \cdot X(H_2) \cdot P_T^2$$

$$\frac{d[H_2]}{dV} = -K_2' \cdot X(C_3H_8) \cdot X(H_2) \cdot P_T^2 - K_1' \cdot X(C_2H_6) \cdot X(H_2) \cdot P_T^2$$

Figure 20. Propane hydrogenolysis: 1st order vs. 2nd order

Table 7. Propane Hydrogenolysis - Effects of Pressure [17]

Ave. Reactor Temp.: 1035°F		Reactor Volume: 0.0636 cu. ft.	
Run No.	15	1	13
Reactor Pressure, psig	500	1000	1500
Feed Rates, lb-mole/hr			
Propane	0.0281	0.0294	0.0281
Hydrogen	0.0557	0.0562	0.0561
Total	0.0838	0.0856	0.0842
Effluent Flow Rate, lb-mole/hr	0.0872	0.0886	0.0861
Effluent Compositions, lb-mole/hr			
C_2H_6, actual	0.00608	0.0102	0.0140
C_2H_6, predicted	0.00666	0.0111	0.0148
H_2, actual	0.0510	0.0490	0.0421
H_2, predicted	0.0490	0.0450	0.0411
CH_4, actual	0.00777	0.0122	0.0166
CH_4, predicted	0.00668	0.0112	0.0151
C_3H_8, actual	0.0223	0.0171	0.0134
C_3H_8, predicted	0.0214	0.0182	0.0132
Rate Constants, lb-mole/hr/psia/ft^3			
1st order: $K_1 \times 10^6$	7.47	7.47	7.47
$K_2 \times 10^4$	6.93	6.33	6.60
2nd order: $K'_1 \times 10^7$	2.18	2.18	2.18
$K'_2 \times 10^5$	3.18	1.57	1.14

runs is described in Figure 21. The model consists of seven irreversible reactions. However, these chemical reactions do not form a linearly independent set because the seventh reaction is a linear combination of the first three.

Originally, a linear independent set consisting of the first six reactions (found in Figure 19) was used to simulate a number of n-butane hydrocracking runs. Effluent yield predictions from these simulations were consistently too low for methane, ethane, ethylene and propane, and consistently too high for n-butane, all relative to the actual results. To reduce the n-butane remaining in the effluent, the chemical reaction $C_4H_{10} + H_2 \longrightarrow 2C_2H_6$ was added to the reaction scheme, thereby destroying the set's linear independence. In addition to reducing n-butane yields, this reaction increased ethane yields -- a desired result.

With this addition to the kinetic model, the n-butane runs were resimulated. Values of the rate constants (K_1 and K_2) for the first and second reactions were calculated using the Arrhenius equations developed for the rate constants of pure ethane and propane hydrogenolysis, respectively. Yet to be determined were the remaining five constants K_3 through K_7.

Chemical Reaction	Reaction Rate Expressions
(1) $C_2H_6 + H_2 \xrightarrow{K_1} 2CH_4$	$R_1 = K_1 \cdot X(C_2H_6) \cdot P_T$
(2) $C_3H_8 + H_2 \xrightarrow{K_2} C_2H_6 + CH_4$	$R_2 = K_2 \cdot X(C_3H_8) \cdot P_T$
(3) $C_4H_{10} + H_2 \xrightarrow{K_3} C_3H_8 + CH_4$	$R_3 = K_3 \cdot X(C_4H_{10}) \cdot P_T$
(4) $C_2H_6 \xrightarrow{K_4} C_2H_4 + H_2$	$R_4 = K_4 \cdot X(C_2H_6) \cdot P_T$
(5) $C_3H_8 \xrightarrow{K_5} C_3H_6 + H_2$	$R_5 = K_5 \cdot X(C_3H_8) \cdot P_T$
(6) $C_4H_{10} \xrightarrow{K_6} C_4H_8 + H_2$	$R_6 = K_6 \cdot X(C_4H_{10}) \cdot P_T$
(7) $C_4H_{10} + H_2 \xrightarrow{K_7} 2C_2H_6$	$R_7 = K_7 \cdot X(C_4H_{10}) \cdot P_T$

Component Rates of Formation

$$d[C_2H_6]/dV = 2 \cdot R_7 + R_2 - R_1 - R_4$$

$$d[H_2]/dV = R_4 + R_5 + R_6 - R_1 - R_2 - R_3 - R_7$$

$$d[CH_4]/dV = 2 \cdot R_1 + R_2 + R_3$$

$$d[C_3H_8]/dV = R_3 - R_2 - R_5$$

$$d[C_2H_4]/dV = R_4$$

$$d[C_4H_{10}]/dV = -R_3 - R_6 - R_7$$

$$d[C_3H_6]/dV = R_5$$

$$d[C_4H_8]/dV = R_6$$

Figure 21. Kinetic Model of n-Butane Hydrogenolysis

In order to determine these unknown rate constants, initial estimates of their values had to be supplied to the numerical routine. The routine then attempted to determine a set of rate constants which provided the most accurate predictions of the effluent yields. The ability of the numerical analysis routine to determine these "best-fit" rate constants was sensitive to the initial estimates of the rate constant values. If the differences between the initial estimates and the best-fit values (which were unknown initially) were many orders of magnitude, then the routine was unable to converge upon the best-fit values, within the constraints of the program.

The determination of five unknown rate constants required a large number of numerical iterations if the initial values of the rate constants were poorly estimated. To improve the efficiency of the routine, the reaction rate expressions R_5 and R_6 for the fifth and sixth reactions, respectively, were assumed to be zero because only small quantities of propylene and butylene were reported in the effluent composition. As a result, only six of the eight formation rates required integration. The initial values of the rate constants K_3 through K_7 were estimated to be equal to those determined by the

Arrhenius expression used for K_2 (pure propane hydrogenolysis). The n-butane runs were simulated and values for K_3 through K_7, less K_5 and K_6, were determined. Using these newly-determined values as initial estimates, the n-butane runs were resimulated without the assumption of zero reaction rates for the propylene and butylene-producing reactions, and the best-fit values for the five rate constants were determined. The final result was a set of rate constants which provided reasonably accurate effluent yield predictions for all components except methane and propane.

The predicted values for methane yields were consistently low while the propane values were high relative to observed results. To remedy this problem, the rate constant K_2 was no longer determined via the Arrhenius expression developed for pure propane hydrogenolysis. Instead, the n-butane runs were resimulated with the rate constant K_2 along with constants K_3 through K_7 to be determined by the numerical routine. The best-fit values previously calculated for K_3 through K_7 were used as initial estimates, while the value for K_2 was initially set equal to that calculated from the propane hydrogenolysis Arrhenius equation. Tables 8a and 8b present a comparison of the actual and predicted values

for the effluent components for ten n-butane runs, while Table 9 lists the best-fit values for K_2 through K_7.

By allowing the rate constant K_2 to be an unknown constant instead of a determinable quantity via the Arrhenius relationship, accurate yield predictions for all effluent components were obtained. However, the kinetic rate constants which produced these good predictions do not exhibit a consistent trend with respect to reactor temperature.

Not one of the rate constants (Table 9) obeys the Arrhenius relationship which predicts exponential increases in the rate constants with increasing reaction temperatures. This additional setback called for a re-assessment of the First-Principles modeling approach.

Table 8a. Butane Hydrogenolysis [17]

Reactor Pressure: 1000 psig			Reactor Volume: 0.0636 cu. ft.		
Run No.	A	B	C	D	E
Reactor Temp., °F	950	1040	1125	1220	925
Feed Rates, lb-mole/hr					
n-Butane	0.01121	0.00930	0.00978	0.01035	0.0233
Hydrogen	0.0315	0.0315	0.0315	0.0306	0.0620
Total	0.04271	0.0408	0.04128	0.04095	0.0853
Effluent Flow Rate, lb-mole/hr	0.0431	0.0426	0.0410	0.0419	0.0915
Effluent Compositions, lb-mole/hr					
C_2H_6, actual	0.00224	0.00716	0.0113	0.00913	0.00220
C_2H_6, predicted	0.00225	0.00728	0.0132	0.00904	0.00219
H_2, actual	0.0274	0.0218	0.0141	0.0100	0.0634
H_2, predicted	0.0279	0.0202	0.0170	0.0099	0.0585
CH_4, actual	0.00332	0.00950	0.0151	0.0225	0.00384
CH_4, predicted	0.00333	0.00946	0.0107	0.0219	0.00383
C_3H_8, actual	0.00233	0.00290	0.00025	0.00004	0.00201
C_3H_8, predicted	0.00234	0.00294	0.00024	0.00004	0.00201
C_2H_4, actual	0.00030	0.00017	0.0	0.00017	0.00018
C_2H_4, predicted	0.00030	0.00017	0.0	0.00017	0.00018
C_4H_{10}, actual	0.00677	0.00089	0.00008	0.00004	0.0186
C_4H_{10}, predicted	0.00689	0.00090	0.00007	0.00004	0.0188
C_3H_6, actual	0.00043	0.00008	0.0	0.0	0.00064
C_3H_6, predicted	0.00043	0.00008	0.00027	0.00009	0.00064
C_4H_8, actual	0.00013	0.00004	0.00004	0.0	0.00037
C_4H_8, predicted	0.00013	0.00004	0.00004	0.00012	0.00037

Table 8b. Butane Hydrogenolysis [17]

Reactor Pressure: 1000 psig			Reactor Volume: 0.0636 cu. ft.		
Run No.	F	K	G	H	I
Reactor Temp., °F	1015	1115	935	1030	1100
Feed Rates, lb-mole/hr					
n-Butane	0.0223	0.0241	0.0454	0.0467	0.0471
Hydrogen	0.0629	0.0623	0.1252	0.1239	0.1244
Total	0.0852	0.0864	0.1706	0.1706	0.1715
Effluent Flow Rate, lb-mole/hr	0.0926	0.0901	0.1788	0.1767	0.1733
Effluent Compositions, lb-mole/hr					
C_2H_6, actual	0.0116	0.0264	0.00358	0.0200	0.0496
C_2H_6, predicted	0.0121	0.0255	0.00358	0.0204	0.0503
H_2, actual	0.0502	0.0277	0.1255	0.0938	0.0520
H_2, predicted	0.0446	0.0267	0.1207	0.0917	0.0511
CH_4, actual	0.0158	0.0341	0.00572	0.0283	0.0632
CH_4, predicted	0.0160	0.0326	0.00572	0.0286	0.0632
C_3H_8, actual	0.00648	0.00153	0.00286	0.0145	0.00590
C_3H_8, predicted	0.00678	0.00153	0.00286	0.0149	0.00591
C_2H_4, actual	0.00130	0.00027	0.00125	0.00177	0.00104
C_2H_4, predicted	0.00131	0.00027	0.00125	0.00177	0.00104
C_4H_{10}, actual	0.00537	0.00009	0.0370	0.0145	0.00087
C_4H_{10}, predicted	0.00567	0.00009	0.0377	0.0150	0.00087
C_3H_6, actual	0.00083	0.0	0.00179	0.00212	0.00017
C_3H_6, predicted	0.00084	0.00088	0.00179	0.00213	0.00017
C_4H_8, actual	0.00018	0.0	0.00036	0.00071	0.00017
C_4H_8, predicted	0.00018	0.00117	0.00036	0.00071	0.00017

Table 9. Kinetic Rate Constants for the n-Butane Hydrogenolysis Runs

Run No.	E	G	A	F	H	B	I	K	C	D
Reactor Temp, °F	925	935	950	1015	1030	1040	1100	1115	1125	1220
Rate Constants: lb-mole/hr/psia/ft^3										
$K_2 \times 10^4$	6.36	7.84	1.34	10.8	14.8	7.18	66.5	40.4	26.2	60.5
$K_3 \times 10^3$	0.206	0.333	0.229	1.30	2.18	1.09	7.90	5.39	1.58	2.66
$K_4 \times 10^4$	2.25	16.9	1.64	2.54	4.16	0.254	0.853	0.206	0	0.133
$K_5 \times 10^4$	6.94	26.4	2.06	2.15	5.45	0.194	0.408	2.43	1.61	0.724
$K_6 \times 10^5$	2.31	2.29	0.971	2.04	6.78	0.751	3.99	37.0	1.32	4.16
$K_7 \times 10^4$	0.566	1.38	0.853	5.09	7.86	3.83	27.0	18.6	15.4	8.24

D. Summary

At the outset of this design project, a one-year target was set in which to develop a viable kinetic model of the GRH. The failure of the Arrhenius relationship to describe the behavior of the rate constants, in combination with this target date, led to the abandonment of the First-Principles Approach in favor of the Weimer model. Although this decision was justifiable in light of the time constraint, an additional analysis of the First-Principles Approach's limited success was warranted.

Wei and Prater [20] investigated the difficulties in determining the values of rate constants from experimental data. They concluded that although rate constants could be developed for complex systems which would fit a particular set of experimental data, these constants would be inaccurate in predicting the reaction kinetics for experimental data which were not used in evaluating these rate constants. Meaningful values for the rate constants would require an excessively large data set which is exceedingly accurate. Unfortunately, the data available for the First-Principles Approach were limited in number and of unknown accuracy.

Another possibility for the limited success attained is that an irreversible, first-order system is inadequate to

explain GRH kinetic behavior. Most of the literature suggests free radical mechanisms to explain thermal hydrocracking behavior. Sundaram and Froment [18] proposed a kinetic model for ethane cracking which consisted of 49 reactions and 20 species (11 molecular and 9 radical). Shultz [17] postulated a free radical scheme to describe ethane hydrogenolysis. However, he stopped short of developing a quantitative treatment of propane hydrocracking in terms of free radical mechanisms because of the complexity of the system and insufficient literature data on the kinetic rate constants involved. To describe the kinetic behavior inside the GRH in terms of free radical mechanisms, a model of extreme complexity would be required for the feedstocks contemplated.

A mathematical model is the result of a compromise between rigor (model complexity) and the availability of accurate kinetic data. The Weimer model with its extensions was just such a compromise. The failure of the Arrhenius relationship to represent the rate constants for the proposed kinetic model of n-butane hydrogenolysis, a desire not to go into complex, free-radical mechanisms, and the opinion of Wei and Prater were three factors which supported the shift to the simpler Weimer model.

REFERENCES

1. Anselmo, K. J., Air Products and Chemicals, Inc., Allentown, Pennsylvania. Personal Communication, March 1979.

2. *Benning, M. A., "The Development of the Gas Recycle Hydrogenator for the Production of Light Hydrocarbons from Partially Vaporized Crude, Refined and Coal Derived Oils", APCI Technical Memorandum No. 257, November 1976.

3. *Bonnell, L. W., "GRH Effluents via Hanna-Weimer Model, PECO", APCI memo to J. Klosek, 31 August 1978.

4. *Bonnell, L. W., "GRH Model (Ref. 31 August 1978, memo to J. Klosek)", APCI memo to R. F. Weimer, 11 September 1978.

5. Bonnell, L. W., Air Products and Chemicals, Inc., Allentown, Pennsylvania. Personal Communication, March 1979.

6. *"British Gas Corporation Gas Recycle Hydrogenator Data Sheets", Nos. 1-21, British Gas Corporation, Research and Development Division, Midlands Research Station, England, Confidential Technology licensed by APCI, 1970-1976.

7. Dennis, J. E., Jr., "Some Computational Techniques for the Nonlinear Least Squares Problem", in Numerical Solution of Systems of Nonlinear Algebraic Equations, G. D. Byrne and C. A. Hall, Eds., New York: Academic Press, 1973.

8. Hulme, B. L., and Daniel, S. L., "Using STFODE/COLODE to Solve Stiff Ordinary Differential Equations", SAND74-0381, Sandia Laboratories, Albuquerque, New Mexico, December 1974. (Program Available from Argonne Code Center).

9. *Klosek, J., "GRH Kinetic Modeling", APCI memo to J. M. Hanna, 23 August 1978.

10. *Klosek, J., "GRH Kinetic Model", APCI memo to J. M. Hanna, 29 August 1978.

11. *Klosek, J., "GRH Kinetic Model", APCI memo to J. M. Hanna, 5 September 1978.

*Confidential to Air Products and Chemicals, Inc. (APCI)

12. *Klosek, J., "GRH Kinet Model", APCI memo to J. M. Hanna, 19 September 1978.

13. Klosek, J., Air Products and Chemicals, Inc., Allentown, Pennsylvania. Personal Communication, March 1979.

14. *Klosek, J., and Tao, J. C., "The GRH Process to Produce SNG and Petrochemical Feedstock from Gas Oils", Presented at 1978 APCI Technology Symposium, December 5, 1978.

15. Murphy, P.S., and Edge, R. E., "The Hydrogenation of Oils to Gaseous Hydrocarbons", Gas Council Research Comm. GC 88 (1962); J.I.G.E., 3, (1963), pp. 459-481.

16. Pelofsky, A. H., Heavy Oil Gasification, New York: Marcel Dekker, Inc., 1977.

17. Shultz, E. B., Jr., "High-Pressure Thermal Hydrogenolysis of Hydrocarbons", Ph. D. Dissertation, Illinois Institute of Technology, Chicago, Illinois, June 1960.

18. Sundaram, K. M., and Froment, G. F., "Modeling of Thermal Cracking Kinetics. 3. Radical Mechanisms for the Pyrolysis of Simple Paraffins, Olefins, and Their Mixtures", Ind. Eng. Chem Fundam., Vol. 17, No. 3 (1978), pp. 174-182.

19. Thompson, B. H., and Brooks, C. T., "The Production of Methane by the Thermal Hydrogenation of Hydrocarbon Oils", Presented at the 165th American Chemical Society National Meeting, Dallas, Texas, April 8th-13th, 1973.

20. Wei, J., and Prater, C. D., "The Structure and Analysis of Complex Reaction Systems", in Advances in Catalysis, Vol. 13, New York: Academic Press, Inc., 1962.

21. *Weimer, R. F., "GRH Kinetics", APCI memo to W. P. Hegarty, 12 January 1977.

*Confidential to Air Products and Chemicals, Inc. (APCI)

Appendix A

Sample Calculations

The mechanism proposed for GRH reaction kinetics involves the reaction of seven hydrocarbon groups representative of the product stream. These groups only hydropyrolyze into smaller groups. The coefficients of the chemical reactions in the kinetic model are based on the most predominant compound of each hydrocarbon group, for example, propane in the C_3^+ group and ethane in the C_2 group. Also, the coefficients reflect the amount of hydrogen consumed during the reaction.

The A_1 group represents one-ring aromatic compounds such as benzene, toluene and xylene. Of these compounds, benzene is the more abundant. The breakdown of the A_1 group is given by:

$$A_1 \xrightarrow{K_4} 0.769\ C_2 + 0.410\ C_1$$

where C_1 is methane only and C_2 includes ethane and ethylene. In the product stream of the GRH, ethane is usually more abundant than ethylene. The A_1 hydropyrolysis reaction can be rewritten as:

$$C_6H_6 + 7\ H_2 \xrightarrow{K_4} 2\ C_2H_6 + 2\ CH_4$$

The molecular weight of benzene is 78.11 pounds per pound mole. If one pound mole of benzene reacts, the amount of ethane and methane produced, in terms of pound of product per pound of benzene, is:

$$\underline{\text{ETHANE}}: \quad \frac{2\ (30.07\ \text{lb}\ C_2H_6/\text{lb mol})}{78.11\ \text{lb}\ C_6H_6/\text{lb mol}} = 0.769\ \frac{\text{lb}\ C_2H_6}{\text{lb}\ C_6H_6}$$

$$\underline{\text{METHANE}}: \quad \frac{2\ (16.04\ \text{lb}\ CH_4/\text{lb mol})}{78.11\ \text{lb}\ C_6H_6/\text{lb mol}} = 0.410\ \frac{\text{lb}\ CH_4}{\text{lb}\ C_6H_6}$$

The coefficients of the remaining five reactions in the model were developed in a manner similar to that just outlined (See Figure 2). Propane, naphthlalene, anthracene and pyrene are the compounds chosen to represent groups C_3, A_2, A_3 and A_4, respectively, when determining the coefficients.

Sample Calculations

```
      PROGRAM FARITY(INPUT,OUTPUT,TAPE5=INPUT,TAPE6=OUTPUT)
      DIMENSION TITLE(11)
      REAL MW


C     THIS PROGRAM UTILIZES THE WEIMER KINETIC MODEL ALONG WITH THE
C     INITIAL BREAKDOWN CORRELATIONS DEVELOPED BY J. HANNA TO PREDICT
C     GRH EFFLUENT YIELDS.


C     EACH FEEDSTOCK CAN BE CHARACTERIZED BY ITS OWN INITIAL BREAKDOWN.
C     THE FIRST DO LOOP PROVIDES THE CAPACITY TO CALCULATE THE
C     CHARACTERISTIC INITIAL BREAKDOWNS FOR ANY NUMBER,N, OF FEEDSTOCKS.
C     THESE INITIAL BREAKDOWNS CAN BE DETERMINED FROM THE CORRELATIONS
C     WHICH FOLLOW IF THE CARBON/HYDROGEN WEIGHT RATIO (C/H) AND THE
C     MOLECULAR WEIGHT (MW) OF THE FEEDSTOCK ARE KNOWN.
C     THE AMOUNT OF 4-RING AROMATICS (X7) PRESENT IN THE INITIAL BREAK-
C     DOWN IS ASSUMED TO BE NEGLIGIBLE.

      READ(5,10) N
   10 FORMAT(I2)
      DO 15 L=1,N
      READ(5,20) CH,MW
   20 FORMAT(2(F10.3))

C     THE FOLLOWING EQUATIONS ARE THE INITIAL BREAKDOWN CORRELATIONS.

      C1=-0.164*CH+1.83
      C2=-0.184*CH+1.72
      C3=-0.127*CH+1.26
      A1= 0.158*CH-0.77
      A2=-0.00258*MW+1.05
      A3=-0.00143*MW+1.08

C     C1 = (X1+X2+X3)          C2 = (X2+X3)          C3 = (X1+X3)
C     A1 = (X4+X5+X6+X7)                        A2 = X4/(X4+X5+X6+X7)
C     A3 = (X4+X5)/(X4+X5+X6+X7)

C     CALCULATE THE INITIAL BREAKDOWN, LB/LB OF OIL FED.

      X1=C1-C2
      X2=C1-C3
      X3=C1-(X1+X2)
      X4=A1*A2
      X5=A3*A1-X4
      X6=A1-(X4+X5)
      X7=0.0


C     NEGATIVE VALUES FOR THE INITIAL BREAKDOWN DO NOT HAVE ANY
C     PHYSICAL MEANING.  THEREFORE, IF THE VALUES PREDICTED BY THE
C     CORRELATIONS ARE NEGATIVE, THEN THESE VALUES WILL BE SET EQUAL TO
C     ZERO.

      IF(X1.LT.0.0) X1=0.0
      IF(X2.LT.0.0) X2=0.0
      IF(X3.LT.0.0) X3=0.0
      IF(X4.LT.0.0) X4=0.0
      IF(X5.LT.0.0) X5=0.0
      IF(X6.LT.0.0) X6=0.0
      IF(X7.LT.0.0) X7=0.0

C     THE SECOND DO LOOP ALLOWS THE PROGRAM TO PREDICT EFFLUENT YIELDS
C     FOR ANY NUMBER,M, OF GRH RUNS FOR A PARTICULAR FEEDSTOCK WHOSE
C     INITIAL BREAKDOWN HAS BEEN DETERMINED IN THE FIRST DO LOOP.

      READ(5,10) M
      DO 25 J=1,M
      READ(5,30) TITLE
   30 FORMAT(5X,11A4)
C     TIME IS THE REACTOR RESIDENCE TIME IN SECONDS.
C     T IS THE REACTOR TEMPERATURE IN DEGREES FAHR.
      READ(5,40) TIME,T
   40 FORMAT(2(F10.4))
```

```
      DENOM=1.987*(T+460.)

      CALCULATE THE REACTION RATE CONSTANTS, SEC(-1).

      RK2=1.5*10.**13*EXP(-126500./DENOM)
      RK3=8.0*10.**10*EXP(-93500./DENOM)
      RK4=2.0*4.4*10.**8*EXP(-94700./DENOM)
      RK5=5.5**2*10.**5*EXP(-66200./DENOM)
      RK6=1.8*10.**5*EXP(-55300./DENOM)
      RK7=2.*3.4*10.**5*EXP(-60300./DENOM)

      CALCULATE THE REACTOR EFFLUENT YIELDS, LB/LB OF OIL FED.

      W7=X7/(1.+RK7*TIME)
      W6=(X6+0.881*RK7*TIME*W7)/(1.+RK6*TIME)
      W5=(X5+0.719*RK6*TIME*W6)/(1.+RK5*TIME)
      W4=(X4+0.609*RK5*TIME*W5)/(1.+RK4*TIME)
      W3=X3/(1.+RK3*TIME)
      W2=(X2+(0.149*RK7*W7+0.337*RK6*W6+0.469*RK5*W5+0.769*RK4*W4+0.682*
     1RK3*W3)*TIME)/(1.+RK2*TIME)
      W1=X1+(0.410*RK4*W4+0.364*RK3*W3+1.067*RK2*W2)*TIME

      W1= METHANE
      W2= ETHANE/ETHYLENE
      W3= PROPANE/PROPYLENE AND HEAVIER PARAFFINS
      W4= BENZENE/TOLUENE/XYLENE
      W5= NAPHTHALENE AND OTHER 2-RING AROMATICS
      W6= ANTHRACENE AND OTHER  3-RING AROMATICS
      W7=     PYRENE AND OTHER  4-RING AROMATICS

      WRITE(6,60) TITLE
   60 FORMAT(1H1,4X,11A4//)
      WRITE(6,65)
   65 FORMAT(7X,*INITIAL*,11X,*PREDICTED*/6X,*BREAKDOWN*,10X,*EFFLUENT*/
     126X,*YIELDS*//)
      WRITE(6,70) X1,W1,X2,W2,X3,W3,X4,W4,X5,W5,X6,W6,X7,W7
   70 FORMAT(5X,*X1= *,F6.3,8X,*W1= *,F6.3/
     2       5X,*X2= *,F6.3,8X,*W2= *,F6.3/
     3       5X,*X3= *,F6.3,8X,*W3= *,F6.3/
     4       5X,*X4= *,F6.3,8X,*W4= *,F6.3/
     5       5X,*X5= *,F6.3,8X,*W5= *,F6.3/
     6       5X,*X6= *,F6.3,8X,*W6= *,F6.3/
     7       5X,*X7= *,F6.3,8X,*W7= *,F6.3//)
   25 CONTINUE
   15 CONTINUE
      STOP
      END
```

Appendix C

Location of Hydrogasification Data in the References

Feedstock	References
Butane	[6]
Synthetic Fuel	[6]
Natural Gas Condensate	[6]
LDF 115	[6]
LDF 170	[6]
Kerosene	[6]
No. 2 Fuel Oil	[2], [12], [21]
Diesel Oil	[6]
Topped Kuwait Crude Oil Fraction	[9], [11], [12], [21]
Monagas Crude Oil Fraction	[2], [9], [12]
Athabasca Tar Sands Crude Oil Fraction	[2], [10], [12]

IRREGULAR

PAGINATION

Appendix C

Location of Hydrogasification Data in the References

Feedstock	References
Butane	[6]
Synthetic Fuel	[6]
Natural Gas Condensate	[6]
LDF 115	[6]
LDF 170	[6]
Kerosene	[6]
No. 2 Fuel Oil	[2], [12], [21]
Diesel Oil	[6]
Topped Kuwait Crude Oil Fraction	[9], [11], [12], [21]
Monagas Crude Oil Fraction	[2], [9], [12]
Athabasca Tar Sands Crude Oil Fraction	[2], [10], [12]